2014

CDOM optical properties near DWH site, Gulf of Mexico: pot oil spill

Zhi Li
Louisiana State University and Agricultural and Mechanical College

CDOM OPTICAL PROPERTIES NEAR DWH SITE, GULF OF MEXICO: POST OIL SPILL

A Thesis

Submitted to the Graduate Faculty of the
Louisiana State University and
Agricultural and Mechanical College
in partial fulfillment of the
requirements for the degree of
Master of Science

in

The Department of Oceanography and Coastal Sciences

by
Zhi Li
B.S., Ocean University of China, 2009
May 2014

Acknowledgements

I would like to gratefully acknowledge my advisor, Dr. Eurico J. D'Sa, for his patience, kindness and guidance during this study and for help with this manuscript. I am also grateful for the constructive suggestions of my committee members Drs. Kanchan Maiti and John White. I would like to thank Dr. Kanchan Maiti's group for sampling and to my lab mate and friend Ishan Joshi for helpful discussion on my thesis.

Thanks are also extended to my family members including my fiancé, my parents, my sister and brother.

Table of Contents

List of Tables

List of Figures

Abstract

The Deep Water Horizon (DWH) oil spill resulted in the largest accidental release of crude oil in U.S. waters with both short- and long-term effects on the marine environment. Extensive studies conducted immediately following the oil spill in the northern Gulf of Mexico provided greater understanding of the physical processes influencing the distribution of the released oil, including the use of optical detection of polycyclic aromatic hydrocarbons (PAHs), a toxic crude oil fraction in the northern Gulf of Mexico. In this study, the optical properties of chromophoric dissolved organic matter (CDOM) and the concentrations of dissolved organic carbon (DOC) were examined from seawater samples collected during two cruises in April of 2012 and 2013 near the DWH spill site in the northern Gulf of Mexico. During both 2012 and 2013, eddies associated with the Loop Current appeared to strongly influence the hydrography at the study site with deeper mixed-layer depths in 2012 than in 2013. Average DOC concentrations were similar in 2013 (mean 0.96 ± 0.20 mg L^{-1}) in comparison to 2012 (0.85 ± 0.25 mg L^{-1}) with higher levels in the near surface waters than at depths. Absorption and fluorescence properties of CDOM for samples obtained in 2013 revealed both the characteristics and composition of CDOM near the DWH site. Absorption coefficients at 355 nm ($a_{CDOM}(355)$ m^{-1}) used to quantify CDOM in seawater varied over a small range and showed elevated values at depths corresponding to or just below the chlorophyll fluorescence maxima suggesting autochthonous contribution to the CDOM pool. In contrast to river-influenced coastal regions, relationships between CDOM optical properties and salinity were not clear due to the small salinity range in the study region. Excitation-emission matrix fluorescence (EEMs) of CDOM revealed the presence of typical humic-like and protein-like fluorophores. Parallel factor analysis (PARAFAC) of EEMs resulted in four fluorescent components characterized as humic-like (two) and protein-like (two). Higher values of protein-like components both in surface and depth at stations with more elevated surface chlorophyll fluorescence

north of the DWH suggests biological contribution to the CDOM pool and its fluxes to depths with implications to related fluxes of contaminants such as PAHs.

Chapter 1 General Introduction

1.1. Background

Chromophoric or colored dissolved organic matter (CDOM) is defined as the optically measureable component of total dissolved organic matter (DOM) that absorbs light in the ultraviolet to visible range of the electromagnetic spectrum. It is also known as gelbstoff, gilvin, and yellow substance (Coble, 1996, 2007; Del Vecchio and Blough, 2004; Zhang et al., 2007). The definition of dissolved is generally referred to all substances that pass through a 0.2 micrometer filter. CDOM forms a significant component (30%-70%) of the DOM pool in natural waters and is mainly derived from two sources: from terrestrial inputs or from in situ biological activities (such as phytoplankton primary production or its microbial decomposition). In the open ocean, CDOM is mainly generated by in-situ biological activity such as microbial decomposition of organic matter and removed by processes such as photo-oxidation and biological degradation. Variations in the CDOM absorption and fluorescence properties can be used to asses changes in CDOM composition resulting from chemical, biological, physical processes that occur in the water column (Coble, 1996; Del Castillo et al., 1999, Del Castillo and Coble, 2000; Stedmon et al., 2007) such as mixing and advection (Vodacek et al., 1997; Nelson et al., 2004, 2007; Morel et al., 2007; Yamashita and Tanoue, 2008).

CDOM optical measurements are obtained by measuring the intensity of absorption of light or fluorescence emission as a function of wavelength. The absorption spectrum of CDOM shows strong absorption in the UV and decreases exponentially with increasing wavelengths in the visible spectral range. Absorption coefficients (e.g., at wavelengths of 355, 375, or 412 nm) and the slopes of the absorption spectra (e.g., between 300-550 nm, or 275-295 nm spectral range) are used to characterize CDOM absorption properties. Linkages between CDOM absorption coefficients and fluorescence at

specific wavelengths for waters in the U.S. east coast and the Louisiana coast have been reported (Hoge et al. 1993; Green and Blough 1994; Singh et al. 2010). Fluorescence measurements using excitation-emission matrix spectroscopy (EEMs) have been used to identify different classes of fluorophores, variation in CDOM composition, and to trace different sources of CDOM (Coble, 1996, 1998; McKnight et al., 2001). Two main fluorescing groups identified in dissolved organic matter are humic-like and protein-like substances. These two forms can be distinguished on the basis of their solubility in alkali and acids. Mixtures of aromatic and aliphatic compounds derived from decomposition of organic matter are identified as humic-like fluorescence substances, while protein-like substances are associated with in-situ biological activity. Humic-like substances are further characterized by humic acids and fulvic acids mainly differentiated on the basis of their solubility (Harvey et al., 1985). Humic acids are dominated by aromatic compounds whereas fulvic acids are characterized by the dominance of aliphatic content. In general, terrestrially derived organic matter and coastal waters are influenced by humic material while oceanic waters away from land are dominated by fulvic acids (Reddy and DeLaune, 2008).

The Deepwater Horizon Oil Spill (also known as the Gulf of Mexico Oil Spill, BP Oil Spill) was caused by an explosion on April 20, 2010, on the BP operated Deepwater horizon offshore oil platform (28.74 °N, 88.39 °W) in the northern Gulf of Mexico. After the explosion and sinking of the Deepwater Horizon oil rig, the sea-floor oil gusher released oil at a depth of 1,544 m and kept flowing for 87 days, until it was capped on 15 July 2010. The Deepwater Horizon Oil Spill considered as the largest accidental oil spill in the U.S. waters, according to the estimates from the federal government's Flow Rate Technical Group, released more than 200 million gallons (or 800 million liters) of crude oil into seawater ("U.S. Scientific Teams Refine Estimates of Oil Flow from BP's Well Prior to Capping," August 2, 2010).

To minimize damage from the oil spill, several approaches were used, such as containment booms, use of chemical dispersants, oil burning and removal. For example, over 4,200,000 feet (1,300 km) of containment booms were deployed to confine the oil flow and protect the Louisiana coastal wetlands, while skimmers were used in the cleanup of near shore waters. Over 700,000 gallons (2.65 million liters) of chemical dispersants were injected into the flow of crude oil to neutralize the oil spread and minimize its impact on the marine environments (NRC, 2005) while ~1.4 million gallons (5.3 million liters) of dispersant were applied to the surface during the Deepwater Horizon oil spill between May 15 and July 12, 2010 (www.whitehouse.gov/blog/issues/Deepwater-BP-oil-spill). The application of dispersants on the surface can increase degradation rate of crude oil and restrain the formation of large emulsions or slicks which are harmful to sensitive coastal environments (Kujawinski et al., 2011). Due to concerns associated with the release of such enormous quantity of oil and gas in the marine environment of the northern Gulf of Mexico, many studies have been conducted to examine the transport, transformation, and fate of the crude oil and its short- and long-term impact on the marine ecosystem. Of particular concern was the detection of polycyclic aromatic hydrocarbons (PAHs), a fraction of the released oil due to its toxicity to marine life and persistence in the environment. Although gas chromatography-mass spectrometry (GC-MS) is the most widely used technique for the detection and measurement of oil hydrocarbons including PAHs, it is costly and time-consuming (Christensen and Tomasi, 2007). Due to their aromatic structure, PAHs have inherent fluorescent properties in the UV spectral range (200-400 nm) (Tedetti et al. 2010). As such, CDOM fluorescence using either single excitation/emission wavelengths or EEMs fluorescence were used in the detection of oil in the Gulf of Mexico following the DWH oil spill (Diercks et al. 2010 Zhou et al. 2012).

The influence of physical processes such as the Loop Current, eddies, currents and winds on the transport of the oil from the DWH site in surface waters were examined using data from multiple

satellites (sea surface temperature (SST) from GOES-East Geostationary, true-color imagery from MODIS ocean color sensor, and synthetic aperture radar (SAR) from Radarsat-2) (Walker et al. 2011). Satellite data revealed the merging of eddies along the Loop Current margin that led to increased circulation area and intensity that also resulted in the rapid offshore entrainment of the surface oil. The presence of a continuous plume of oil more than 35 kilometers in length, at approximately 1100 meters depth that persisted for months without substantial biodegradation was observed during vertical sampling including long-range surveys with an autonomous under-water vehicle (Camilli et al. 2010). EEMs fluorescence of seawater samples collected during the DWH oil spill used in conjunction with PARAFAC modeling detected six fluorescence components with half of them being associated with crude or weathered oil (Zhou et al. 2013).

The oil spill was unique due to the enormous amount of crude oil and chemical dispersants released into the environment and the uncertainty of their fate. Physical and biological processes in the Gulf, such as stratification, euphotic depth, dissolved oxygen, and wind field were important factors determining the oil and the chemical dispersant's fate in the marine environment. Although the DWH oil spill occurred in 2010, its impact in the open ocean and the coastal waters have persisted for a much longer period (Lin and Mendelssohn, 2012; Mendelssohn et al., 2012) suggesting the need to continue monitoring the northern Gulf of Mexico for potential effects of the DWH accident on the seawater biogeochemical properties including DOM/CDOM optical properties. Seawater samples collected during two research cruises in 2012 and 2013 enabled as part of this study to examine the post-spill CDOM absorption and fluorescence properties and DOC concentrations at locations close to the DWH oil spill site.

1.2. Study Area

The northern Gulf of Mexico is one of the main regions for oil and gas development in the U.S. It provides ~23 percent of total U.S. crude oil production and seven percent of total U.S. natural gas production (Gulf of Mexico Fact Sheet, http://www.eia.gov/). The Mississippi and Atchafalaya Rivers annually discharge about 580 km^3 of water and 210 billion m^3 of sediment (Milliman and Meade, 1983) into Gulf of Mexico. This discharge strongly influences the biogeochemical properties of the northern Gulf. The Deepwater Horizon Oil Spill (28.74 ℃N, 88.39 ℃W) that occurred in the northern Gulf of Mexico on April 20, 2010 is considered as the largest oil spill in the U.S. waters. As part of a post-spill study, two survey cruises were conducted in April 2012 and 2013 near the DWH site (Figure 2.1). During both cruises, sampling stations were located near DWH site with eight CTD and water sampling stations in 2012 and four sampling stations during the 2013 cruise. Overall, the sampling stations were grouped as nearshore and offshore based on their relative positions from the coast and the DWH spill site. Water samples obtained at these stations at various depths were processed for DOC concentrations for the 2012 cruise and for DOC concentrations and CDOM absorption and fluorescence properties for the 2013 cruise.

1.3. Absorption and Fluorescence Spectroscopy

CDOM absorption spectra typically show an exponentially decreasing trend with increasing wavelength in the UV and visible spectral range (Zepp and Schlotzhauer 1981; Blough et al, 1993) and can be modeled by an exponential equation as a function of wavelength (λ) as:

$$a(\lambda) = a(\lambda_0) exp^{[s(\lambda_0)-\lambda]} \quad (1)$$

where, $a(\lambda)$ is the absorption coefficient and S is the slope of the exponential curve. The absorption coefficient a is calculated from the absorbance A spectra obtained from measurements using a

spectrophotometer. The dimensionless absorbance spectra is then converted to absorption coefficient (m^{-1}) at each wavelength λ, using the equation:

$$a(\lambda) = 2.303 \times \frac{A(\lambda)}{l} \quad (2)$$

where A(λ) (calculated as (Log (I_0/I), I is the intensity) is the absorbance at a wavelength λ, l is the path-length in meters. The CDOM absorption coefficient at 355 nm, $a_{CDOM}(355)$ is used to represent the concentration or amount of CDOM in seawater. The spectral slope (S, nm^{-1}, or μm^{-1}) is generally calculated by taking a fit of least square regression of a_λ versus wavelength over a specific spectral range (e.g., 275 to 295 nm range) and can provide information on the source and nature of the CDOM (Helms et al. 2008).

Fluorescence measurements have also been used to characterize CDOM due to their greater sensitivity (Green and Blough 1994). Although correlation between CDOM fluorescence and absorption has been reported, their magnitude and spectral dependence are sensitive to factors such as pH, the presence of quenchers and composition (Blough and Del Vecchio 2002). Fluorescence excitation emission matrix spectroscopy (EEMs) which measures CDOM fluorescence of emitted light as a function of excitation wavelength, has been widely used to identify different classes of fluorophores, variation in CDOM composition, and to trace different sources of CDOM in fresh and oceanic waters (Coble, 1996, 1998; McKnight et al., 2001). Different fluorophores within CDOM will fluoresce when excited by UV and visible light at different wavelengths. The EEMs was obtained by running the samples on a Horiba Jobin Yvon Fluoromax-4 spectrophotometer system (equipped with a 50 W ozone-free Xenon arc lamp and a R928P photomultiplier tube as a detector). The Fluoromax-4 spectrophotometer was set for scanning in ratio mode with dark offsets. Excitation spectra was from 250

to 500 nm at 5 nm intervals while emission spectra was recorded between 290 – 600 nm at 5 nm intervals.

Parallel factor analysis (PARAFAC) is a statistical modeling approach that is used to decompose a dataset of EEMs into mathematically and chemically independent components that represent a single fluorophore or a group of strongly covarying fluorophores. PARAFAC analysis of an EEMs dataset results in a reduction of three-dimensional dataset into a set of two-dimensional spectra representing chemically independent components that describe the total EEM (Stedmon et al. 2003).

1.4. Objectives

The purpose of this study was to examine the DOC concentrations and CDOM optical properties in conjunction with the physical properties in the ocean water near the Deepwater Horizon site following the spill. We test the hypothesis that the CDOM spectral absorption and fluorescence properties near the DWH site mainly reflect the influence of the Loop Current waters and associated eddies. In order to test the above hypothesis, data collected during CTD casts (profiles of temperature, salinity, oxygen, and chlorophyll fluorescence) along with properties of water samples collected at discrete depths (DOC concentrations, CDOM absorption and fluorescence) during survey cruises in April of 2012 and 2013 are studied to characterize the CDOM and their relationships to physical and biological properties. Specifically, the hydrography at the study site, the physical and biological influences on CDOM absorption and fluorescence properties, and the fluorescence signatures related to PAHs if any, are examined.

Chapter 2 Physical Properties near DWH Site, Gulf of Mexico in 2012 and 2013

2.1. Introduction

The northern Gulf of Mexico is one of the main regions for oil and gas development in the U.S. It provides ~23 percent of total U.S. crude oil production and 7 percent of total U.S. natural gas production (Gulf of Mexico Fact Sheet, http://www.eia.gov/). In April 2010, Deepwater Horizon Oil Spill, which is considered as the largest oil spill accident in U.S. waters, released more than 200 million gallons (or 800 million liters) of crude oil into seawater (Mascarelli, 2010; Schrope, 2011). As part of response action, over 700 thousand gallons (2.65 million liters) of chemical dispersants were injected into the flow of oil and in surface waters of the Gulf (Kujawinski et al., 2011). The oil spill was unique due to the enormous amount of crude oil and chemical dispersant released into the environment and the uncertainty of their fate.

The Loop Current and its associated eddies along with wind forcing played an important role in the transport of the surface oil during the DWH oil spill (Walker et al. 2011). The wind field and entrainment of the oil in the LC eddies were found to strongly influence the motion of oil toward and off the coastal region. Following the oil spill, a continuous oil plume at ~1100 m depth extended for more than 35 kilometers in length near the DWH site was observed that persisted for months without substantial biodegradation (Camilli et al. 2010). A significant increase in bioavailable PAHs at four coastal sites, namely, Grand Isle-Louisiana, Gulfport-Mississippi, Gulf Shores-Alabama, and Gulf Breeze-Florida was also observed following the DWH accident (Allen et al. 2012). Although the DWH oil spill occurred in 2010, its impact on the Gulf ecosystem has persisted for a longer period (Lin and Mendelssohn, 2012; Mitra et al. 2012). Physical and biological processes such as currents, stratification, euphotic depth, dissolved oxygen, and winds are important factors determining the transport and fate of particulate and dissolved organic matter including pollutants in the marine environment. In this chapter

the general physical properties in the northern Gulf of Mexico are examined using satellite derived sea surface height (SSH) anomaly and sea surface temperature (SST) in conjunction with water column hydrographic properties for the period corresponding to the 2012 and 2013 survey cruises near the DWH site.

2.2. Methods

The sampling stations were located near DWH site in the northern Gulf of Mexico (Figure 2.1) during two week-long cruises in April 2012 and 2013 conducted onboard the R/V Walton Smith. There were eight sampling stations (blue drops) during the 2012 cruise (9-16 April) and four sampling stations (yellow circles) during the 2013 cruise (4-15 April). These stations could be grouped as nearshore and offshore relative to the coast and the DWH site. The sampling stations were named by a capital letter (N or O) to represents nearshore or offshore, followed by a number (2 or 3) to represent cruise in 2012 or 2013; the end number represents the distance from DWH site to the sampling stations (larger number mean larger distance).

The main instrument package used during the cruises for obtaining profiles of water column biophysical properties was the SBE 9plus (SeaBird Electronics, Inc.). The SBE 9plus unit was used for continuous measurement of conductivity, temperature and depth (pressure) at a frequency of 24 Hz (24 scans per second) during vertical profiling operations. The SBE 9plus unit uses the modular SBE 3plus temperature sensor, SBE 4 conductivity sensor, SBE 5T submersible pump, and the SBE 32 carousel water sampler (for triggering sample bottles).

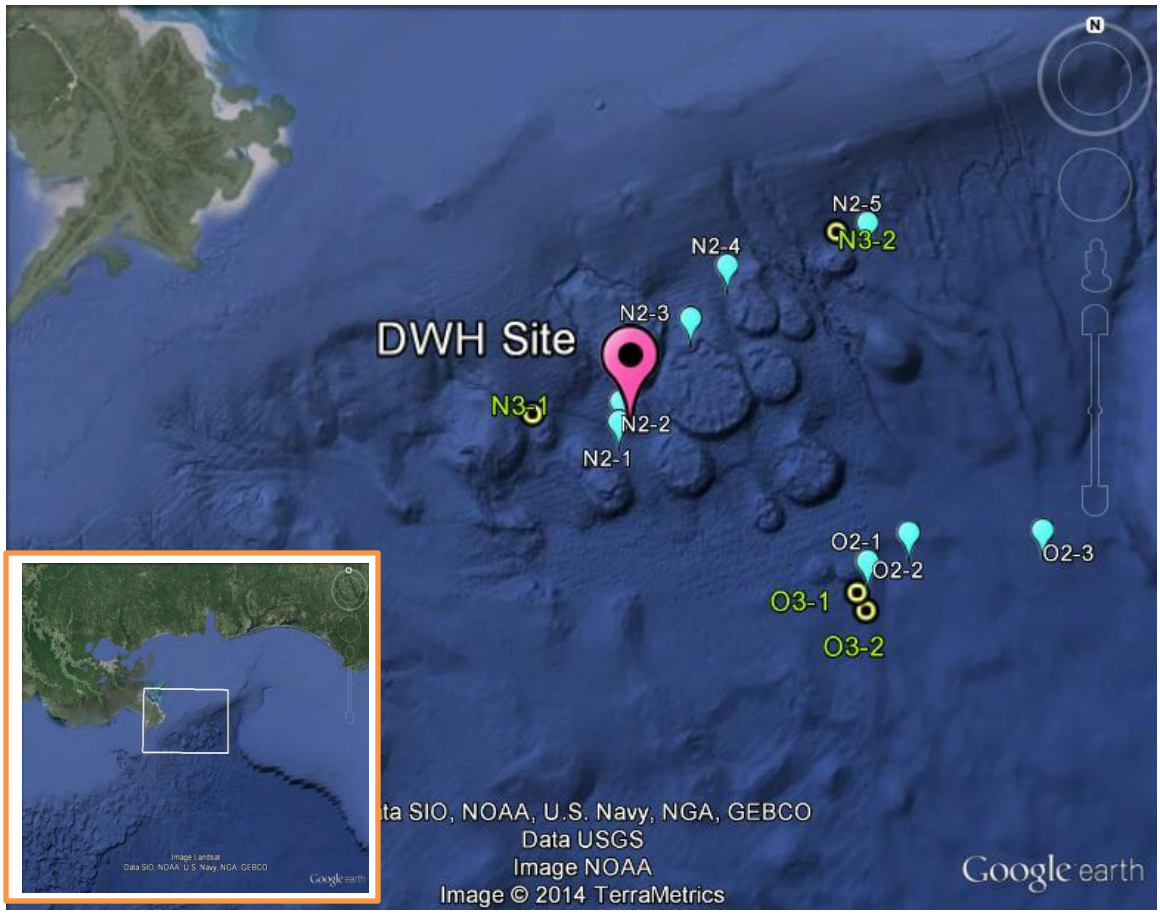

Figure 2.1 Study area showing the station locations near the DWH site for the 2012 cruise (blue drops), and the 2013 cruise (yellow circles).

The SBE 3plus temperature sensor provides temperature measurement in a range of -5 to 35 ^{O}C with an accuracy of ± 0.001 ^{O}C. The SBE 4 conductivity sensor from which salinity is derived measures conductivity in the range 0 to 7 Siemens/meter with an accuracy of +/- 0.0003 S/m. Separate sensors have been incorporated in the CTD unit to measure dissolved oxygen and chlorophyll fluorescence. The SBE 43 sensor used for dissolved oxygen has a measurement range of 120% of surface saturation in all natural waters with an accuracy of 2% saturation. Chlorophyll-a fluorescence is an important indicator of active phytoplankton abundance and chlorophyll concentrations. Fluorescence measurements were obtained with a WETStar fluorometer (WET Labs) attached to the CTD unit. It provides chlorophyll-a measurement in the range of 0.03 – 75 µg/L with a sensitivity of 0.03 µg/L. Two profiles have been

acquired for each CTD cast, one for downcast (descending) and another for upcast (ascending). In the present study only the downcast profile data have been used as generally the upcast profile data are noisier due to water disturbance.

Sea surface height (SSH) is the height of the sea surface above a known reference surface, such as the earth's ellipsoid or the marine geoid. SSH is computer from satellite altimeters using the altimeter range and its altitude above the reference ellipsoid. SSH anomalies represent the difference between the best estimate of the sea surface height and a mean sea surface (Leben et al. 2002). SSH anomaly contour plots for April 15, 2012, and April 15, 2013 were downloaded from Colorado Center for Astrodynamics Research website (http://eddy.colorado.edu/ccar/ssh/hist_global_grid_viewer) and are shown overlaid on GOES sea surface temperature (SST) satellite data.

2.3. Results and Discussion

2.3.1 General Physical Properties of the Study Area

The Mississippi and Atchafalaya Rivers annually discharge about 580 km^3 of water and 210 billion m^3 of sediment (Milliman and Meade, 1983) into Gulf of Mexico, which constitutes 10% of the total water mass on the Texas-Louisiana and Mississippi-Alabama continental shelves (Dagg, 1990) and 55% of the total freshwater input to the gulf (Solis and Powell, 1999). Due to the high discharge from the Mississippi River off the birdsfoot delta, coupled with interactions with Loop Current eddies and wind forcing, modeling studies show that the freshwater discharged by the Mississippi River are often entrapped by the eddies – toward the east and offshore under the influence of currents associated with ocean mesoscale eddies (Morey et al. 2003).

Winds and Loop Current eddies are important factors that influence the coastal circulation and the offshore dispersal of freshwater from the Mississippi/Atchafalaya Rivers. Wind stress plays a

significant role in driving the coastal waters to create continental shelf flows in northern Gulf of Mexico (Sturges 1993). Consistent seasonal wind patterns will tend to establish consistent seasonal scale current patterns (Johnson, 2008). Based on wind stress and resulting surface currents, a summer season (June, July and August) and a non-summer season comprising remainder of the year has been proposed for the northern Gulf of Mexico (Cho et al. 1998). This general wind pattern (Figure 2.2) where in the wind stress is toward the west/southwest for non-summer months, and northwestward during the summer months, strongly influences the onshore or offshore dispersal of waters.

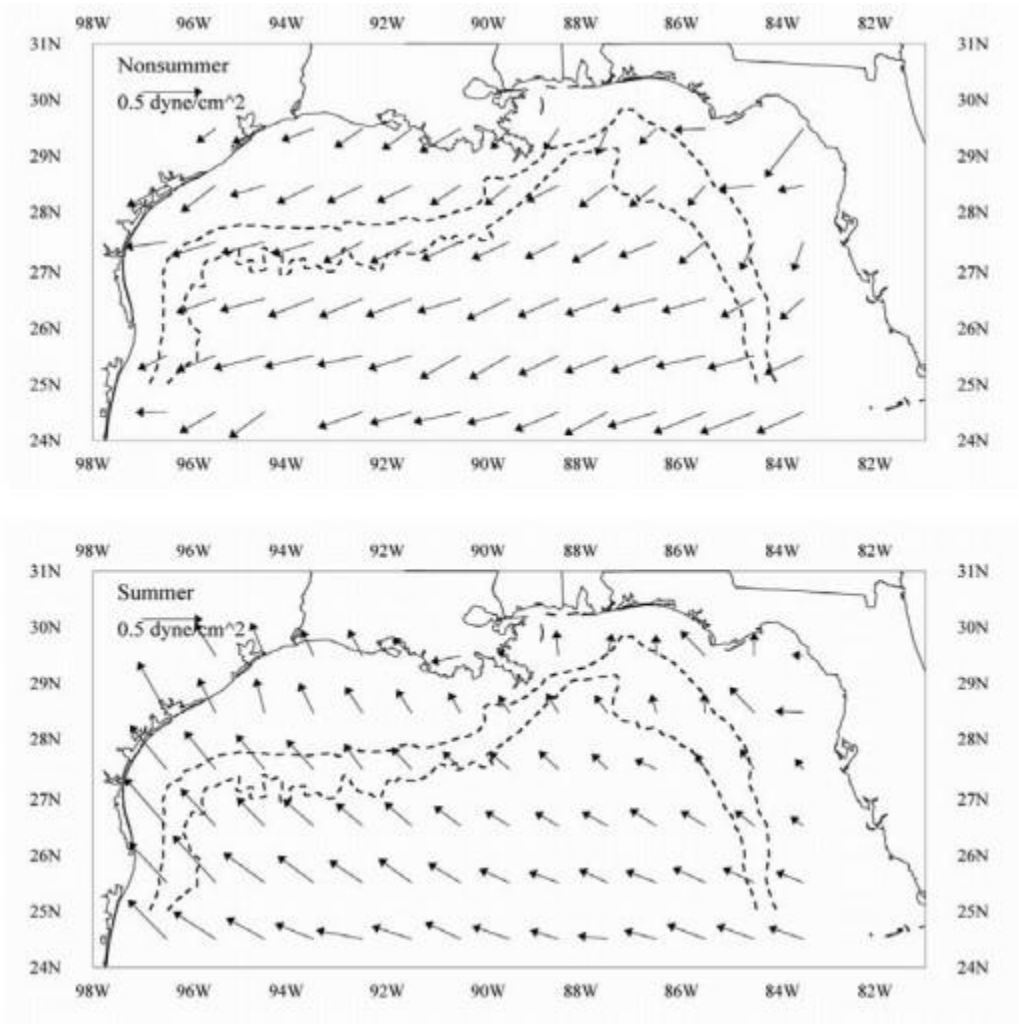

Figure 2.2 Average wind stress for non-summer (upper) and summer (lower) months. (Johnson, 2008)

The Loop Current is a significant feature in the Gulf of Mexico that brings warm waters from the Caribbean into the Gulf. The Loop Current is a clockwise stream that spreads into the northern Gulf of Mexico that couples the Yucatan Current and the Florida Current (Hofmann and Worley, 1986). The position of Loop Current is variable often intruding northward in the Gulf of Mexico and periodically shedding eddies that move slowly to the west-southwest at a speed of about 3-5 km per day; this eddy also known as a Loop Current eddy or a warm core ring rotates clockwise due to the Coriolis force (Collow, 2010). The eddy shedding cycle, which typically ranges from 6 to 11 months is a gradual process (Sturges and Leben, 2000). Cold core rings generally smaller in size than the warm core rings appear to form along the boundary of the Loop Current or the boundary of the warm core rings (Vukovich 2007). Offshore transport of Mississippi River plume waters east of the delta have been observed in ocean color satellite data that were initiated by winds and plume interactions with eddies (Nababan et al. 2011).

2.3.2 Physical Properties during the 2012 Cruise

The SSH anomaly contour plot overlaid on GOES satellite sea surface temperature (SST) for April 15, 2012 and corresponding to the sampling period of the 2012 cruise shows the Loop Current extending up to ~27.5° N into the northern Gulf of Mexico (Figure 2.3). The warm Loop Current water enters the Gulf of Mexico through the Yucatan Channel and exits through the Straits of Florida. The frontal boundary of the Loop Current generally penetrates as far north as 27° usually prior to a warm core ring separation, which is about 20% of the time (Vukovivh 2007). Just above the Loop Current is what appears to be a remnant of a clockwise rotating warm core eddy. The nearshore stations appear to lie within or at the edge of the remnant warm core eddy, while the offshore stations were within the cooler shelf waters entrapped within the clockwise rotating eddy (Figure 2.3).

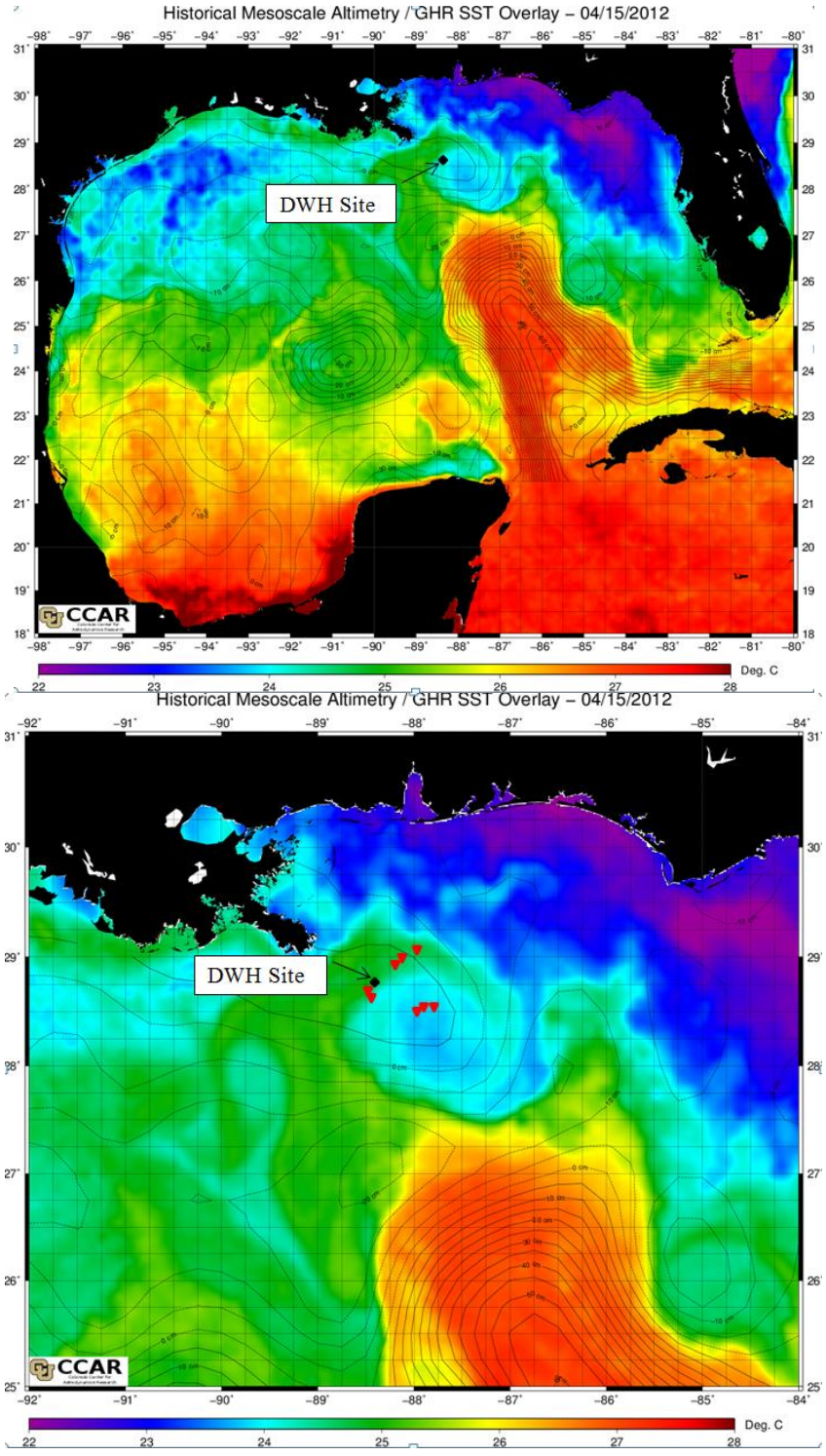

Figure 2.3. SSH anomaly contours overlaid on SST image of the Gulf of Mexico and Caribbean waters for April 15, 2012.
(http://eddy.colorado.edu/ccar/ssh/hist_gom_grid_viewer)

Vertical profiles of temperature, salinity, chlorophyll fluorescence, and dissolved oxygen for the eight sampling stations during the April 2012 cruise include the five nearshore stations (N2-1 to N2-5) and the three offshore stations (O2-1 to O2-3) (Figure 2.4). While salinity appeared uniform within the mixed layer, temperatures were warmer in the surface and decreased with depth within the mixed layer.

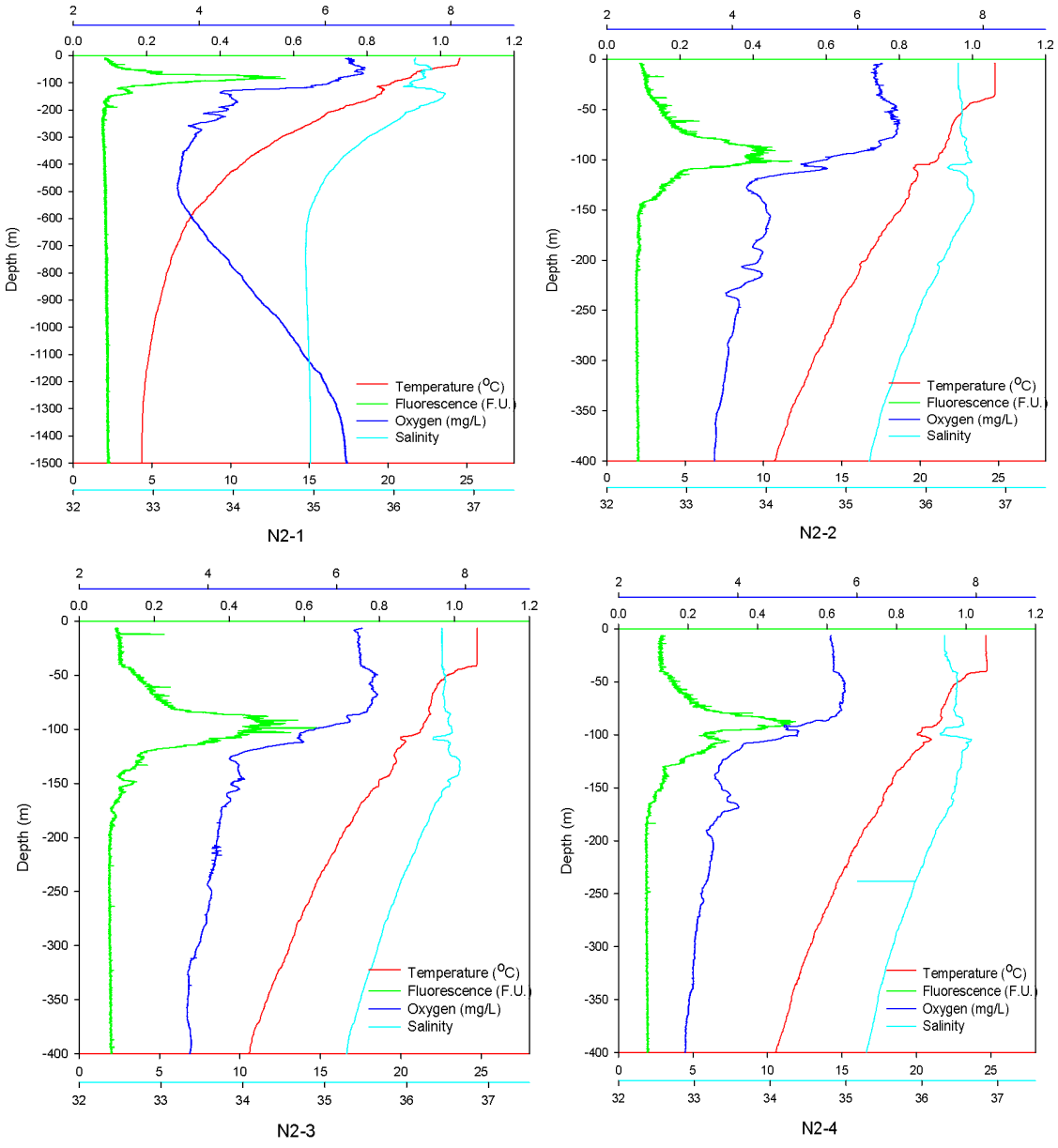

Figure 2.4 Vertical profiles of temperature, salinity, chlorophyll fluorescence, and dissolved oxygen for the eight stations sampled during 2012.

(Figure 2.4 continued)

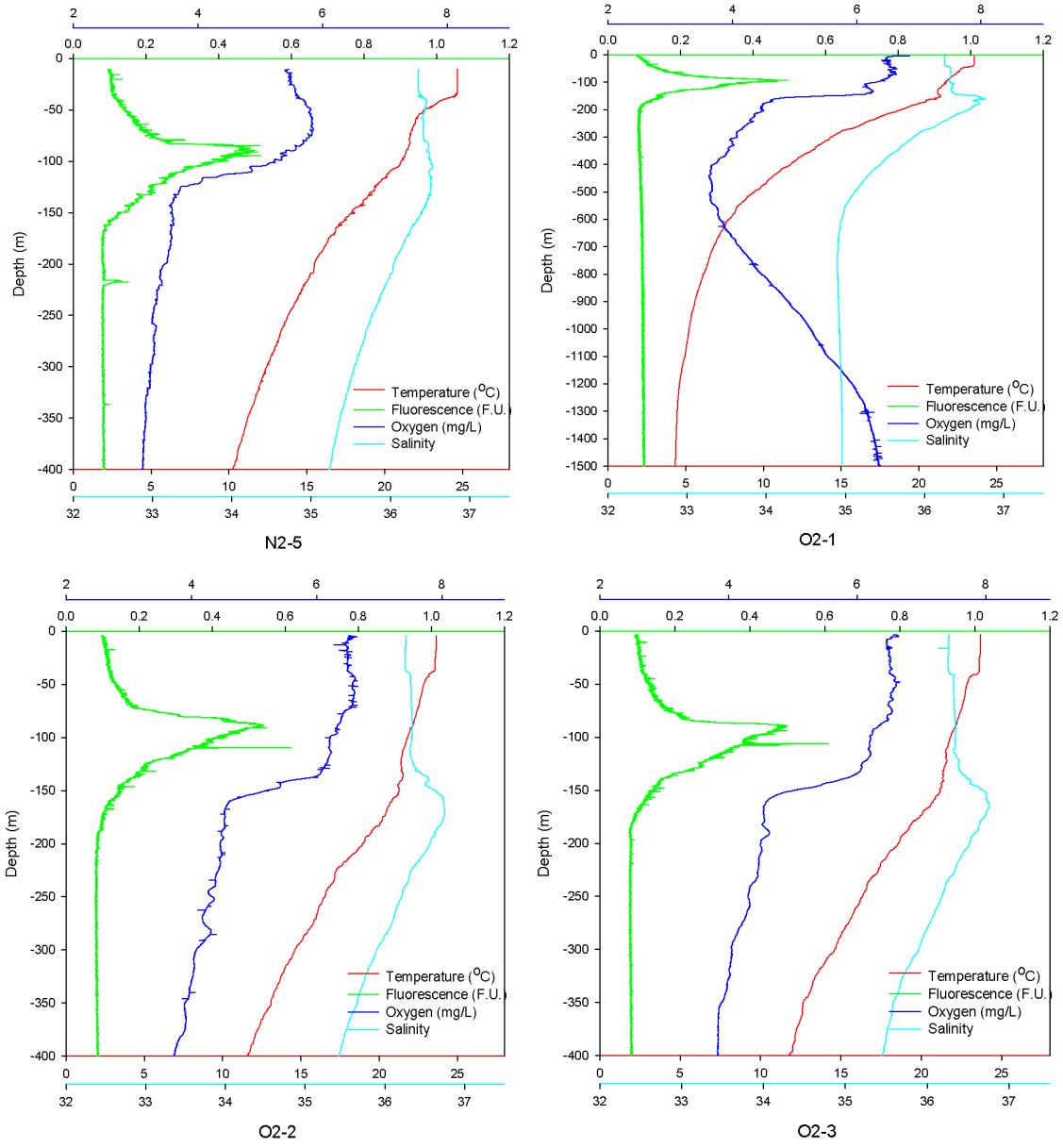

Below the mixed layer, temperature decreased with depth, while salinity increased slightly at ~160 m before decreasing with depth. At all stations, chlorophyll-fluorescence peaks were observed at the base of the mixed layer. Dissolved oxygen is elevated within the surface mixed layer and increased with depth associated with increasing phytoplankton biomass as indicated by the chlorophyll fluorescence profile. Variability at depth below the chlorophyll maximum is likely due to respiration associated with sinking organic matter. The oxygen minimum layer observed between 200-400 m at all the stations is a

feature that is associated with water masses entering the Gulf as part of the Loop Current (Morrison and Nowlin, 1977).

Although the vertical profiles of temperature and salinity at the eight stations generally appear similar (Figure 2.4) with a warm, fresher surface mixed layer, there were clear differences between the nearshore and offshsore stations. Average surface temperature and salinity for the nearshore stations was 24.67 ^{o}C and 36.35, respectively. At 750 m depth which was the bottom layer for near shore stations, average temperature and salinity was 6.23 ^{o}C, and 34.90, respectively. For near shore stations, the average chlorophyll fluorescence maxima were located at ~88 m depth. Chlorophyll fluorescence peaked at ~ 84 m for N2-1 and N2-5, and ~91 m for N2-2 to N2-4.

Average surface temperatures at the offshore stations were slightly cooler (23.68 ^{o}C), while the average surface salinity was slightly lower (36.27) than the nearshore stations. These differences in temperature and salinity between the nearshore and offshore waters can be explained by the satellite derived SSH and SST imagery (Figure 2.3) which reveals the presence of warm, and higher salinity warm core eddy waters occupying the area of the nearshore stations while the colder waters occupied the offshore stations. Overall, these different water masses did not influence the biological productivity in the surface waters likely due to low nutrient levels in these two water masses. At depth 750 m, the average temperature and salinity was 7.02 ^{o}C and 34.91, respectively, and were not much different from the nearshore stations.

2.3.3 Physical Properties during the 2013 Cruise

The SSH anomaly contour plot overlaid on sea surface temperature (SST) for April 15, 2013 (Figure 2.5) corresponding to the survey cruise near the DWH site in 2013 reveals the Loop Current to be extending only up to about 25° N latitude. A large anti-cyclonic warm core eddy that likely recently

separated from the Loop Current occupied the region south of the DWH site. Over the DWH site, a cyclonic cold core eddy appeared to be present that entrapped a cooler plume of shelf waters on its northwestern edge that likely influenced the properties of the nearshore stations close to the DWH site. This plume of cooler water that extends from the shelf to approximately the DWH site likely influenced the water properties at the nearshore stations.

The temperature, salinity, chlorophyll fluorescence, and dissolved oxygen profiles at the four sampling stations during the 2013 include two nearshore stations (N3-1 and N3-2) and offshore stations (O3-1 and O3-2) (Figure 2.6). Overall, the temperature and salinity profiles at the four stations sampled during 2013 survey cruise appeared very similar with main differences in the physical properties being in the surface waters. At near shore stations, salinity was slightly lower than the two offshore stations indicating the influence of shelf waters extending offshore (Figure 2.5). At N3-1, a strong chlorophyll fluorescence peak appears at 38 m with a corresponding drop in oxygen. Although an increase in oxygen would be expected due to photosynthesis, enhanced respiration associated with secondary production may be contributing to the reduced oxygen levels at these depths. At station N3-2, a sharp but reduced chlorophyll fluorescence peak was observed at the same depth as that of station N3-1 indicating similar but reduced shelf water influence as this station appeared to be located at the edge of the shelf plume waters (Figure 2.5). However, a second broad chlorophyll fluorescence peak at 72 m was similar to the two offshore stations. Although surface salinity appear similar between the nearshore and offshore stations, the small but distinct differences suggest the water masses at these stations are likely different. The high chlorophyll fluorescence at station N3-1 suggests higher nutrient levels likely associated with shelf plume waters extending offshore near the DWH site station.

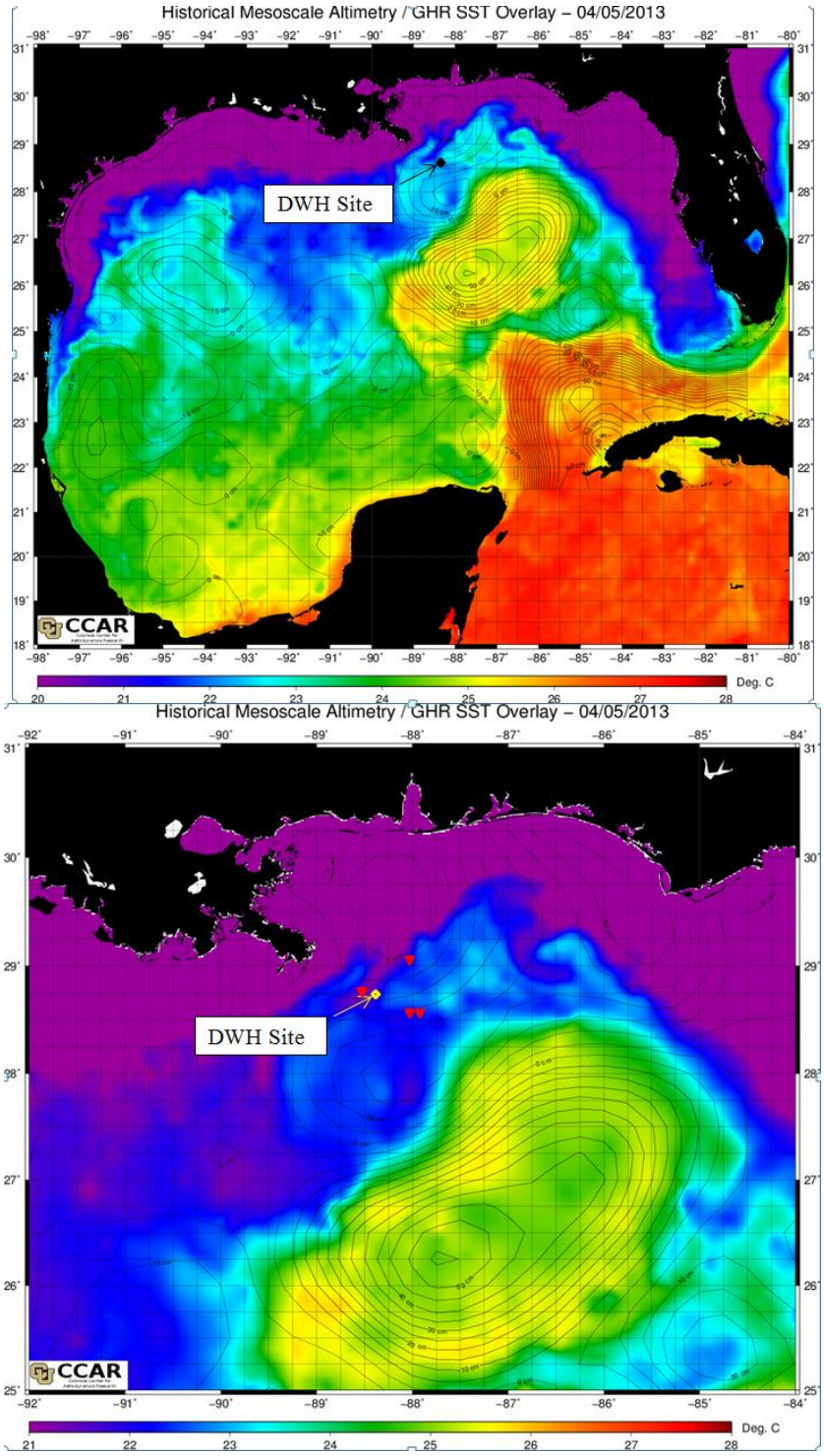

Figure 2.5. SSH anomaly contours overlaid on SST image of the Gulf of Mexico and Caribbean waters for April 15, 2013. (bottom) Same image expanded to show the station locations. (http://eddy.colorado.edu/ccar/ssh/hist_gom_grid_viewer)

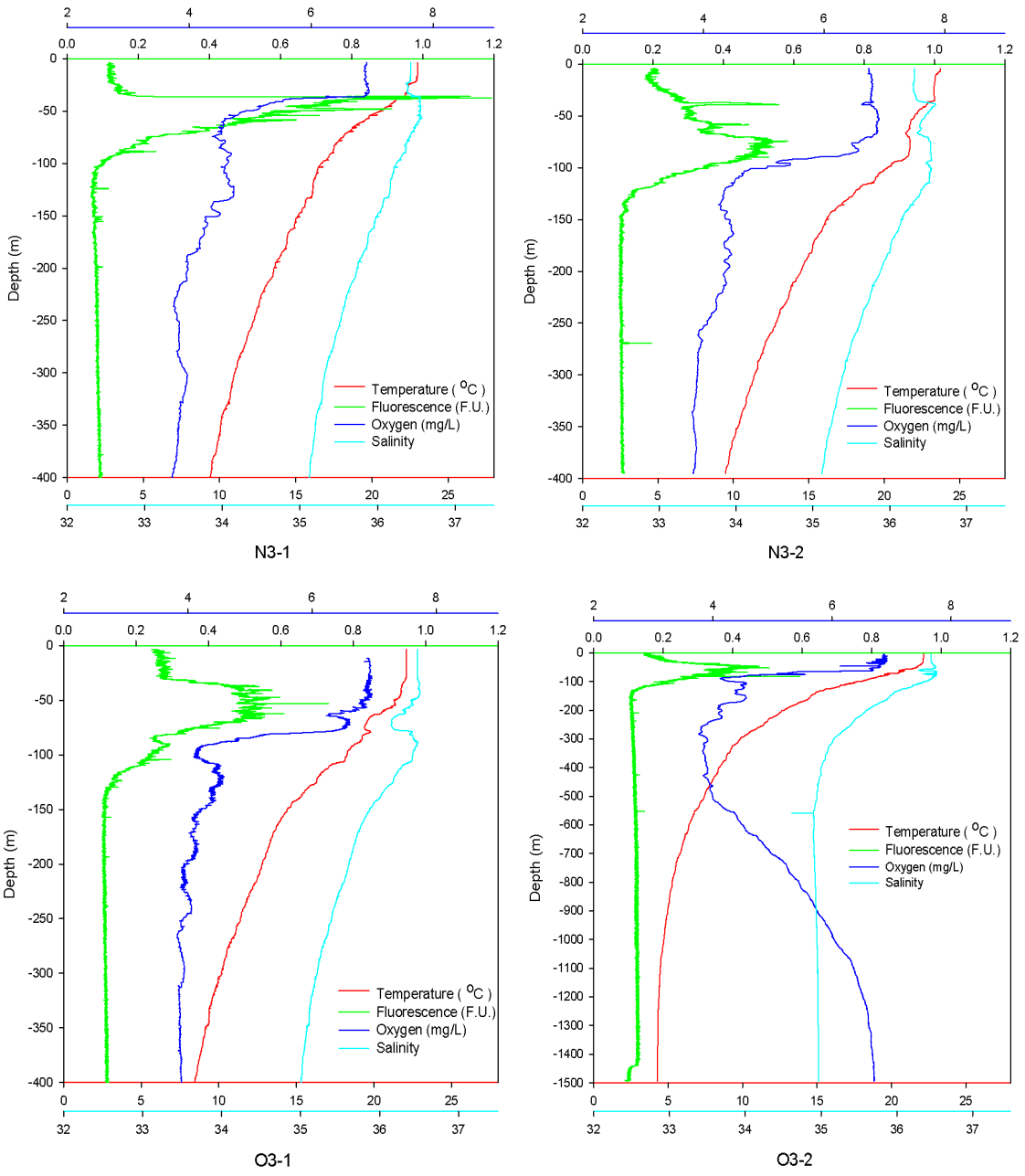

Figure 2.6 Vertical profiles of temperature, salinity, chlorophyll-a fluorescence, and dissolved oxygen at the four sampling stations in April 2013.

Although the mixed layer depth while variable appeared to be shallower in 2013 than during the 2012 survey, the overall levels of chlorophyll fluorescence and concentrations of dissolved oxygen appeared similar likely suggesting similar levels of dissolved organic material near the DWH site during the two survey years.

Chapter 3 DOC and CDOM Properties near DWH Site, Gulf of Mexico-Post Spill

3.1. Introduction

Chromophoric/Colored dissolved organic matter (CDOM) is defined as the optically measurable component of total dissolved organic matter (DOM) that absorbs light ranging from ultraviolet to visible electromagnetic spectrum. CDOM forms a siginificant component (30%-70%) of the DOM pool in natural waters and is mainly derived from terrestrial sources or from in situ production. In the open ocean, CDOM is mainly generated by in-situ biological activity such as microbial decomposition of organic matter. CDOM can be removed due to photo-oxidation or by biological degradation. Variations of the CDOM absorption and fluorescence can be a proxy of changes in CDOM composition resulting from chemical, biological, physical processes that occur in the water column (Coble, 1996; Del Castillo et al., 1999, Del Castillo and Coble, 2000; Stedmon et al., 2007; D'Sa and DiMarco, 2009). CDOM properties have been studied using their absorption and fluorescence properties. CDOM absorption is strong in UV and exhibits an exponentially decreasing intensity with increasing wavelength in the visible spectral range (Del Vecchio and Blough, 2006). The two main fluorescing groups identified in dissolved organic matter are humic-like and protein-like substances. Fluorescence spectroscopy using EEMs (excitation-emission matrix) has been widely used to characterize CDOM in various water masses (Del Castillo et al., 1999; Del Castillo and Coble, 2000).

EEM fluorescence spectroscopy enables the measurements of an assembly of fluorescence emission spectra that is collected over a range of excitation wavelengths for a CDOM sample and is used to provide information on the relative intensity of fluorescence for different excitation-emission wavelength pairs. Due to different fluorescence features of different fluorophores present in CDOM, fluorescence maximum localization has been used identify different fluorophores in CDOM (Coble 1996). These include the humic-like A, C, and M peaks, and the protein-like T and B peaks (Table 3.1).

The T-peak represents the tryptophan-like amino acid and the B peak the tyrosine-like amino acid. The wavelength ranges for the excitation and emission peaks and their corresponding designation are shown in Table 3.1. The analysis of a large number of EEMs data using peak-picking techniques on individual EEMs can be time-consuming. PARAFAC analysis of a large EEM dataset results in a reduction of the three-dimensional data into several two-dimensional spectra that represent the independent components that describe the total EEM (Stedmon et al. 2003).

Table 3.1 Coble (1996) defined fluorescence peak locations at excitation wavelength and maximum fluorescence emission intensity.

Fluorescence Peaks	Excitation(nm)	Emission(nm)	Coble's Designation (1996)
UV-C Humic like	260(250-260)	380-480	A peak
UV-C Humic like	350(330-350)	420-480	C peak
Marine Humic like	312(310-320)	380-420	M-peak
Tryptophan like, protein like	275(270-280)	340(320-350)	T peak
Tyrosine-like, protein like	275(270-280)	310(300-320)	B peak

The Deepwater Horizon Oil Spill event in April 2010 resulted in the release of more than 200 million gallons (or 800 million liters) of crude oil into seawater (Mascarelli, 2010; Schrope, 2011). Further, as part of response action, over 700 thousand gallons (2.65 million liters) of chemical dispersant were injected into the flow of oil and in surface waters of the Gulf (Kujawinski et al., 2011). The oil spill was unique due to the enormous amount of crude oil and chemical dispersant released into the environment and the uncertainty of its fate. Physical and biological processes in the Gulf were found to be important in determining the transport and fate of the spilled in the northern Gulf of Mexico (Walker et al. 2011). Various measurements including DOC concentrations and CDOM fluorescence were used to detect oil in seawater during the oil spill event (Diercks et al. 2010; Zhou et al., 2013). Although the DWH oil spill occurred in 2010, its impacts have been shown to persist for much longer period (Lin and

Mendelsohnn, 2012). In this chapter the DOC distribution and CDOM optical properties are examined in the water column at locations near the DWH spill site for seawater samples collected during survey cruises in April of 2012 and 2013.

3.2. Methods

3.2.1 Study Area

Water sampling was conducted near the DWH site in the northern Gulf of Mexico for the two cruises in April 2012 and 2013 (Figure 3.1). There were eight sampling stations (blue drops) during the 2012 survey cruise and samples were analyzed only DOC concentrations. For the 2013 cruise there were four stations (yellow circles) and samples were analyzed for both DOC concentrations and CDOM absorption/fluorescence measurements. These stations could be grouped as nearshore or offshore stations based on their relative distance from the coast and the location of the DWH site.

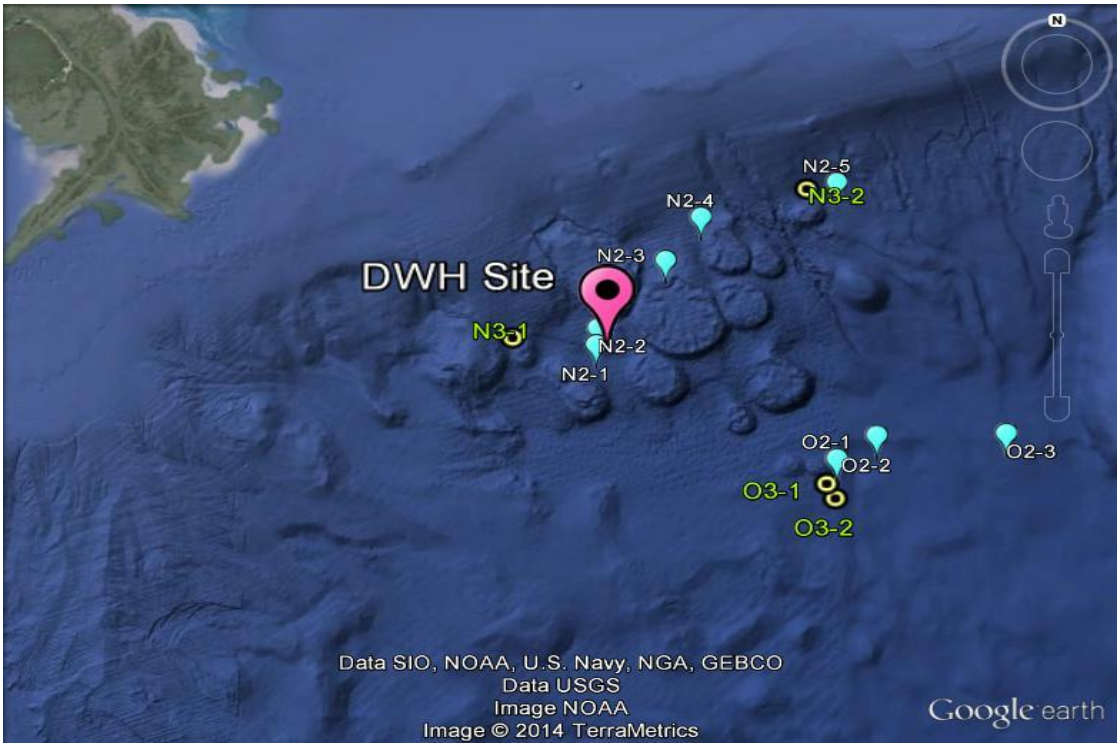

Figure 3.1 Sampling locations near the DWH site. Stations sampled during 2012 are indicated by blue drops and by yellow circles for the 2013 cruise.

3.2.2 Sample Collection

Water sampling was conducted at 8 stations for DOC measurements in 2012 and at 4 stations around DWH site in 2013 for DOC and CDOM optical measurements with samples collected at various depths from Niskin bottles during the CTD casts. The water samples were immediately filtered onboard using pre-rinsed 0.2 μm nucleopore membrane filters and stored in a refrigerator at 4 ℃. These samples were then brought back to the laboratory for optical absorption and fluorescence analyses. Milli-Q from a Barnstead Nanopure® Model D-50280 purification system was used as reference water.

3.2.3 DOC Concentrations

Dissolved organic carbon or DOC is a primary measure of the total dissolved organic matter (DOM) present in natural waters. Samples for DOC were collected in pre-combusted amber colored glass bottles with Teflon-lined caps. Samples were processed for DOC on a Shimadzu TOC-5000A analyzer.

3.2.4 Absorption Measurements

Water samples stored in the refrigerator at 4 °C were allowed to reach room temperature before conducting the absorption and fluorescence measurements on a spectrophotometer and a spectrofluorometer. A multipath capillary waveguide system used for absorption measurements was switched on ~30 minutes before the samples were analyzed to warm-up and stabilize the instrument. The capillary waveguide cell was rinsed by three cleaning solutions before running samples (Miller et al. 2002). Absorption spectra were obtained between 190 and 722 nm at 1-nm intervals using the waveguide set to 50 cm path length. Each sample was run three times, and two closest absorbance spectral sets were used in the analysis. For the reference, salt solutions with refractive indices close to seawater samples were prepared using granular NaCl (Mallinckrodt) and Milli-Q water. This procedure is required to minimize the differences in refractive index between sample and reference that cause

offsets in absorbance measurements (D'Sa et al. 1999). The absorption coefficients (a) were calculated from the absorbance (A) obtained from the spectrophotometer using:

$$a(\lambda) = 2.303 \times \frac{A(\lambda)}{l} \quad (3)$$

where, A(λ) (calculated as (Log (I_0/I), I is the intensity) is the absorbance at a wavelength λ, l is the path-length in meters. The absorption coefficient at 355 nm ($a_{CDOM}(355)$) was used to quantify CDOM absorption in seawater. Spectral slope coefficients (S, μm^{-1}) were calculated by taking a fit of least square regression of the plot a_λ versus wavelength over the range 375 to 395 nm (Helms et al., 2008).

3.2.5 Fluorescence Measurements

Water samples were treated in the same way as in absorption measurements before fluorescence measurements on a Horiba Jobin Yvon Fluoromax-4 spectrophotometer system. This instrument which is equipped with a 50 W ozone-free Xenon arc lamp and a R928P photomultiplier tube as a detector was switched on 30 minutes before the samples were analyzed to stabilize the instrument. Samples were not diluted to account for inner filter effects as the absorbance of all the samples all less than 0.2 at 250 nm ($A_{250} < 0.2$). Nanopure Milli-Q water was used as blank and water scans obtained before and after a set of measurements were made. The Fluoromax-4 spectrophotometer was set to scanning ratio mode with dark offsets. Emission spectra were obtained between 290 – 600 nm at 5 nm intervals over an integration time of 0.1s while the excitation spectra was from 250 to 500 nm at 5 nm intervals. Factory supplied correction factors were applied to correct for sample scanning. Milli-Q water blank EEMs were subtracted from the sample EEMs to eliminate Raman peaks.

3.2.6 PARAFAC Analysis

PARAFAC analysis was applied using a modified MATLAB toolbox developed by Colin Stedmon (NERI, Aarhus University, Denmark). The method of Stedmon et al. (2003, 2008) was used to

evaluate PARAFAC constraints, such as non-negativity, and model initialization values derived from singular value decomposition (SVD). PARAFAC determination of the numbers of CDOM components was done by split-half analysis and resolution of loadings and minimization residuals, which was applied to the EEM dataset (28 samples) with some statistical assumptions as reported by Stedmon et al. (2003, 2008).

PARAFAC statistically decomposes the three-way data into individual fluorescence components or moieties with a least square regression. Bro (1997) has demonstrated the uniqueness of PARAFAC decomposition method to reduce an EEM into tri-linear term and a residual array.

$$X_{ijk} = \sum_{n=1}^{F} a_{in} b_{jn} c_{kn} + \varepsilon_{ijk} \quad (4)$$

where, for EEM fluorescence data, X_{ijk} is the fluorescence intensity of the i^{th} sample at the k^{th} excitation and j^{th} emission wavelength. a_{in} is directly proportional to the concentration of the n^{th} fluorophore (or component F) in the i^{th} sample, b_{jn} and c_{kn} are estimates of emission and excitation spectra of n^{th} fluorophore at wavelength j and k, respectively. F is the number of components and ε_{ijk} the residual matrix of the model that represents unexplained variability by the model (Singh et al., 2010). Split-half analysis of PARAFAF models was performed for validation (Kowalczuk etal. 2009; Stedmon et al. 2007).

3.3. Results and Discussion

3.3.1 Water Column DOC Distribution

Dissolved organic matter (DOC) is a primary measure of the total dissolved organic matter (DOM) present in natural waters. DOC concentrations varied from 0.58 to 1.23 mg/L (mean = 0.85 ± 0.25 mg L^{-1}) in 2012. During 2013 cruise DOC concentrations varied from 0.72 to 1.24 (mean = 0.96 ±

0.20 mg L^{-1}). These values were generally within the range observed in the Gulf of Mexico (Guo et al. 1995) but less than those observed in the Mississippi River plume waters (Guo et al. 2009). However, DOC concentrations during 2012 and 2013 were much lower than those measured during the oil spill event (values as high as 6 mg/L) in 2010 at stations influenced by released oil (Zhou et al. 2013).

The vertical distributions of DOC concentrations for nearshore and offshore sampling stations for 2012 generally exhibited larger values in the surface mixed layer and decreased with depth (Figure 3.2 and Figure 3.3). This pattern has also been reported in a previous study (Guo et al. 1995). However, DOC concentrations decreased at 100 m and for all the inner shelf stations and one outer shelf station DOC increased to higher levels at depths between 350 – 400 m and then decreased to their lowest values at greater depths. This pattern of water column distribution was also observed in PAHs during the same cruise (Adhikari et al. –submitted). The water column DOC distribution during 2013 near the DWH site

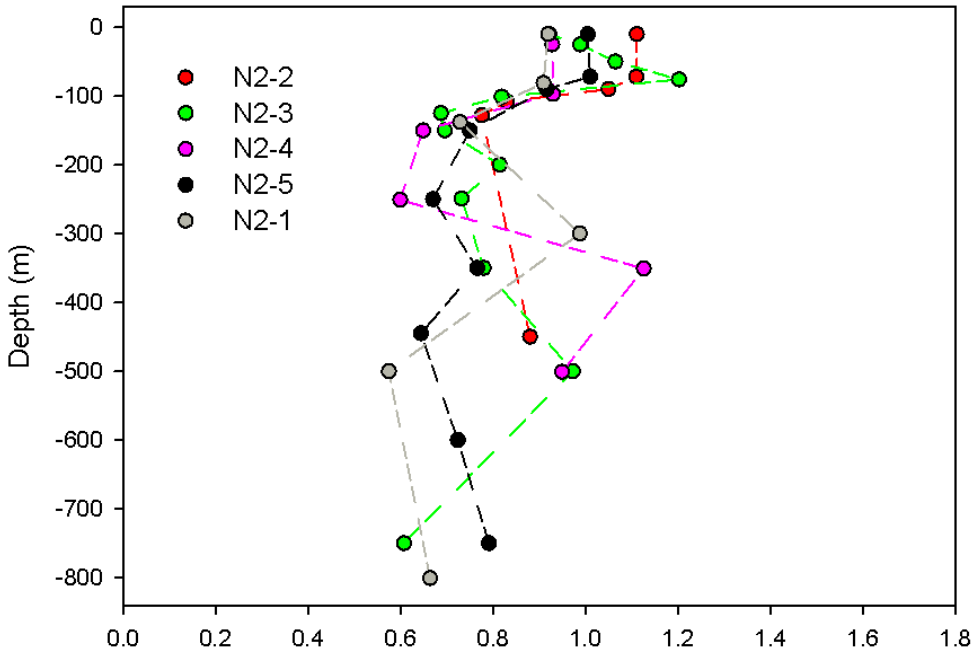

Figure 3.2 DOC concentrations (mg/L) at nearshore stations during April 2012.

(Figure 3.4) was generally higher in the surface mixed layer (Figure 2.4) indicating higher levels of DOC in near-surface waters are likely related to higher biological productivity in these waters.

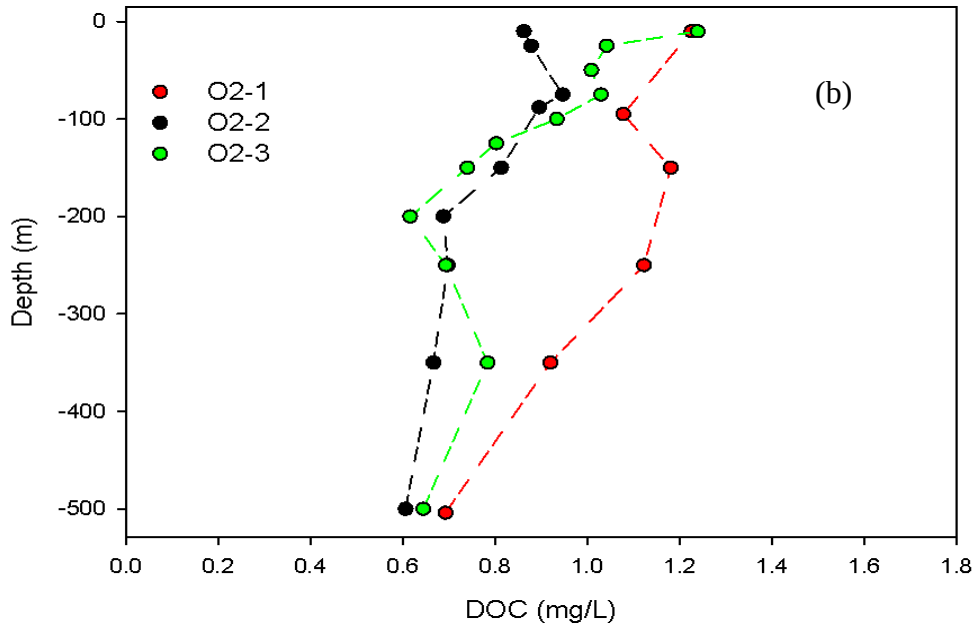

Figure 3.3 DOC concentrations (mg/L) at offshore stations during April 2012.

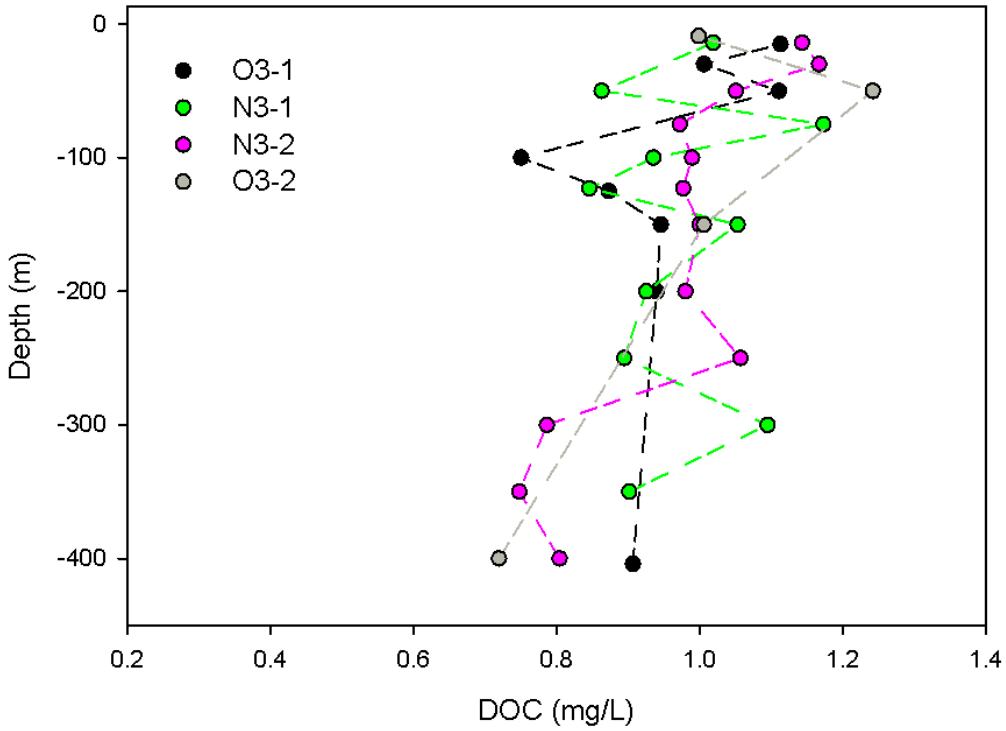

Figure 3.4 DOC concentrations (mg/L) at four stations in April 2013.

3.3.2 CDOM Absorption Properties near DWH Site 2013

Representative CDOM absorption spectra at different depths for the four stations (Figure 3.5) all show absorption typically decreasing exponentially from UV to visible range. Although CDOM absorption did not vary greatly with depths and across the stations, the exponential rate of decrease with increasing depths and stations appear to be variable likely due to differences in water properties or influences on CDOM. Generally, at all the four stations spectra at 15 m and 100 m are higher and have greater rate of decrease in absorption with increasing depth than absorption spectra at greater depths.

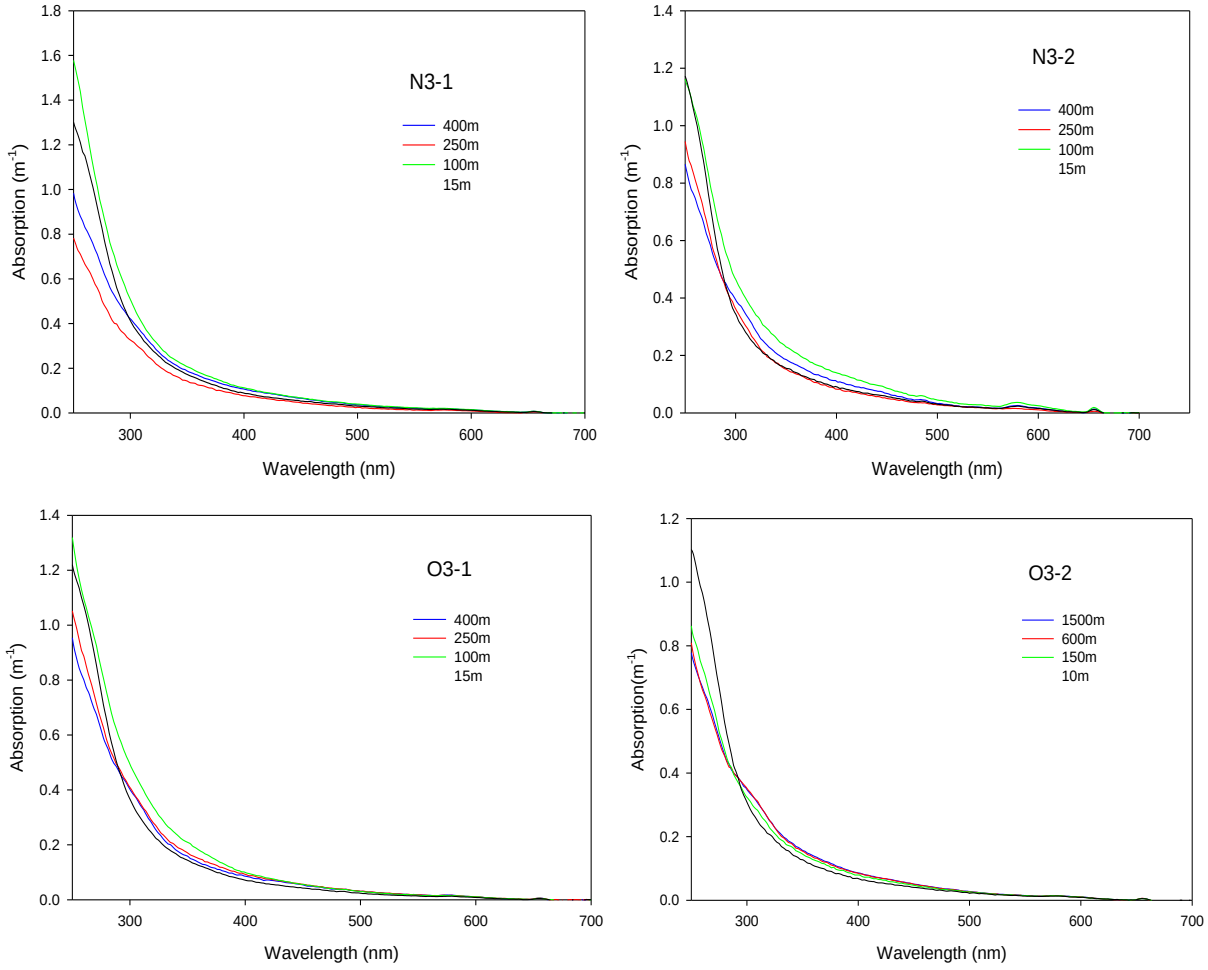

Figure 3.5 CDOM absorption spectra at four different depths for the four 2013 stations

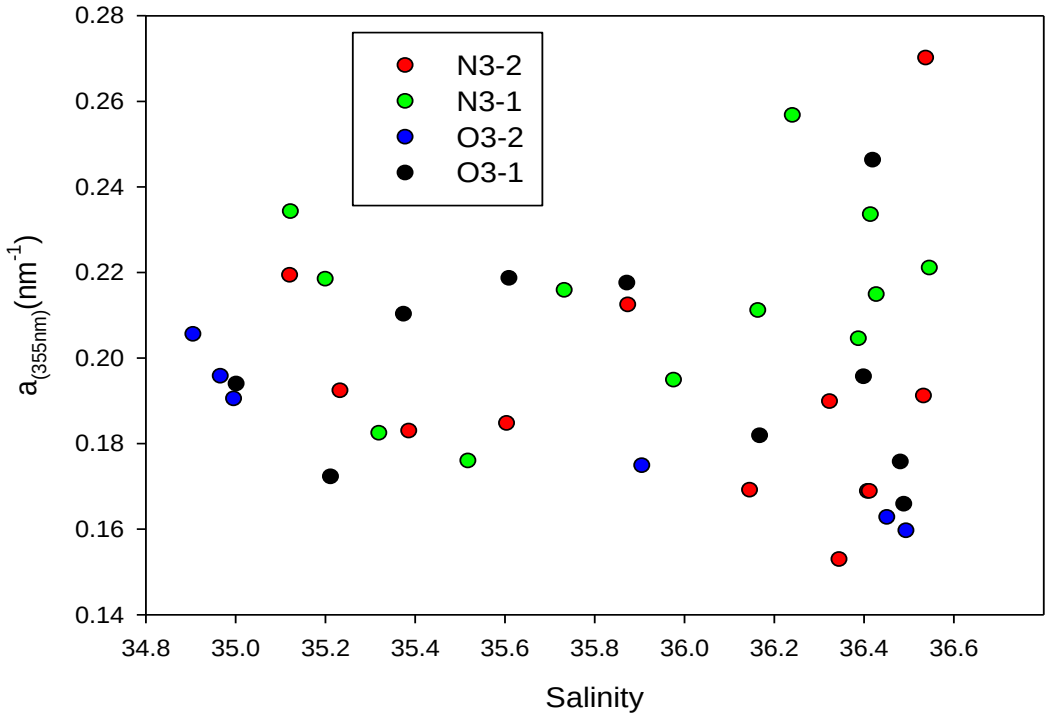

Figure 3.6. CDOM absorption at 355 nm plotted versus salinity.

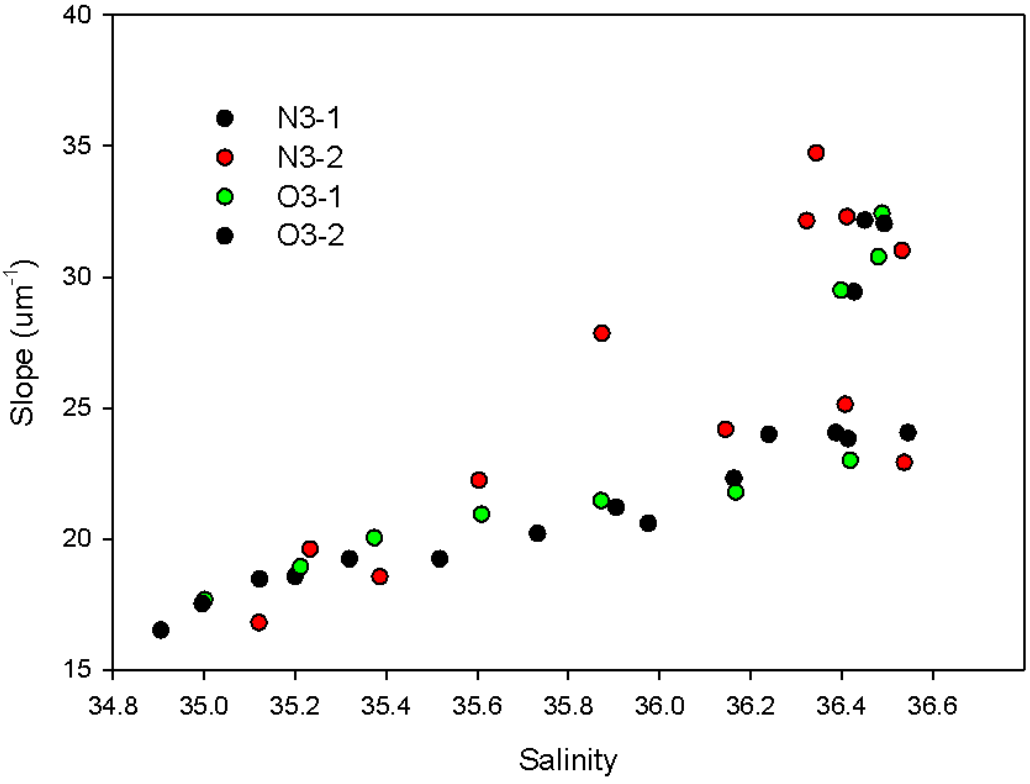

Figure 3.7 Spectral slope (between 275-295 nm) plotted versus salinity.

As the range in salinity at the sampling site is small (0.8), the pattern of CDOM-salinity relationship (Figure 3.6) is not clear in comparison to coastal and river dominated waters where CDOM generally decreases with increasing salinity (D'Sa and DiMarco 2009). CDOM absorption-salinity relationship shows a different pattern for the nearshore and offshore stations (Figure 3.6). Overall, CDOM levels appear lower for the two offshore stations (O3-1 and O3-2) than the inner stations. CDOM is also generally higher at lower salinity with the exception of a few data points. In contrast, CDOM at the two nearshore stations (N3-1, N3-2) are higher over the salinity range than the offshore stations. This elevated CDOM at the nearshore stations is likely associated with the plume of shelf waters detected on the outer edge of the counterclockwise rotating cold core eddy (Figure 2.3). These waters likely contained higher levels of CDOM than the offshelf stations (O3-1, O3-2) which were observed to be located within the cold core eddy (Figure 2.3). Highest values of CDOM were also observed at the two nearshore stations at the high salinity values which were associated with surface waters.

The spectral slope in contrast showed a clear increase in slope values with increasing salinity (Figure 3.7). The spectral slope was lowest at the lowest salinity that corresponded to the highest depth. Spectral slope was highest at the high salinity values that were in the near surface waters. High CDOM spectral slopes have been attributed to photo-oxidation that results in CDOM loss (Helms et al. 2008). Such higher levels in CDOM spectral slopes in surface waters have been reported in other studies in the Gulf of Mexico (D'Sa and DiMarco, 2009; Shank and Evans, 2011).

CDOM absorption at 355 nm which is used to quantify CDOM absorption, shows variability with depth for both the nearshore and offshore stations during 2013 (Figure 3.8). Except for the O3-2 offshore station which is observed to increase with increasing depth, the other stations had lower CDOM in surface that then increased to its maximum at ~100 m depth, with another peak observed at ~200 m.

Levels then decreased and increased again with depth (Figure 3.8). In contrast to DOC concentrations which were higher in surface waters, the lower CDOM levels in surface waters suggest that photo-oxidation losses occurring in the CDOM pool may be associated with a smaller fraction of the dissolved organic matter pool. The peaks in CDOM absorption observed at ~100 m correspond to elevated chlorophyll fluorescence (Figure 2.6) suggesting a biological source of CDOM at this depth.

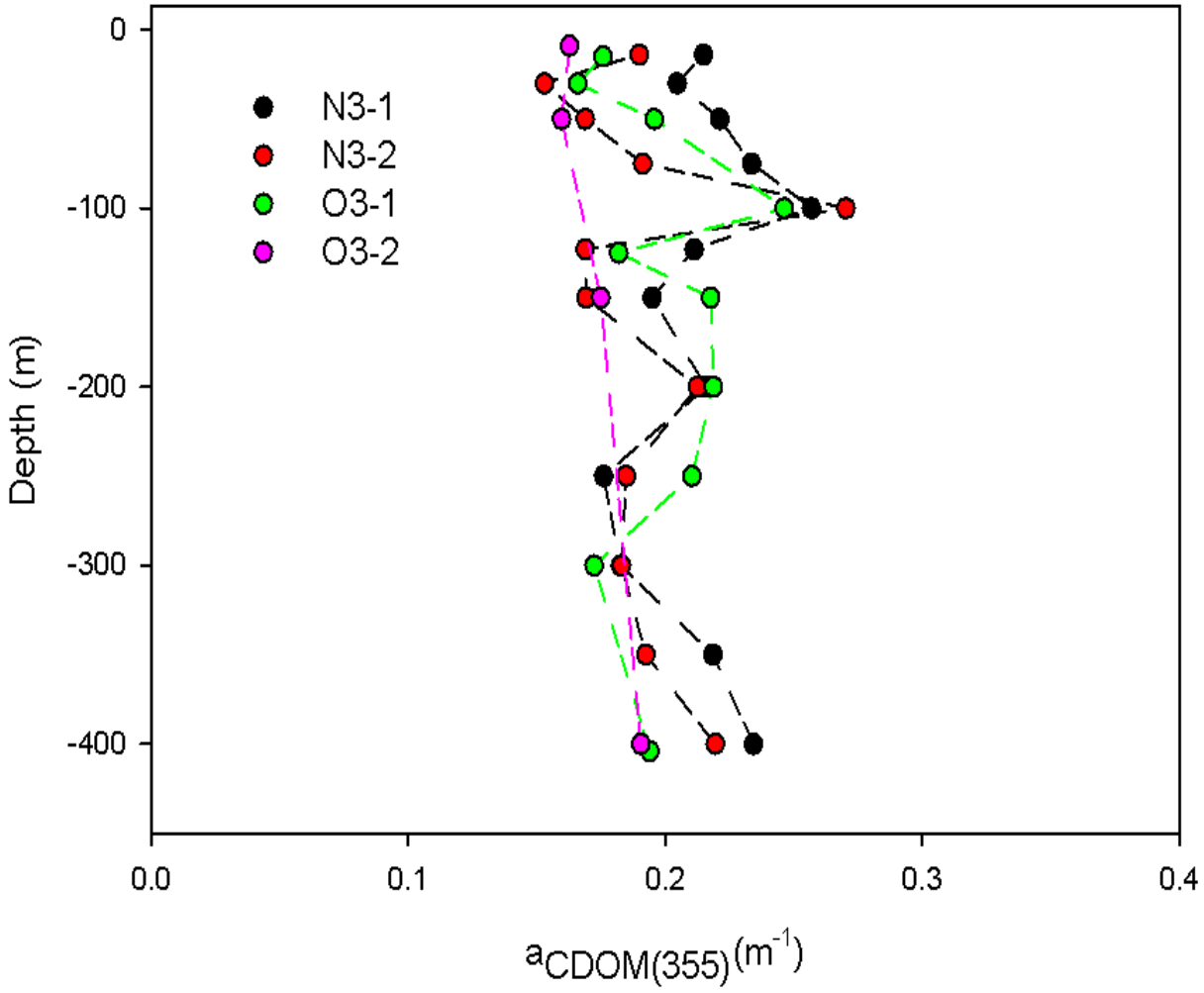

Figure 3.8 CDOM absorption coefficient at 355 nm with depth at four stations for 2013.

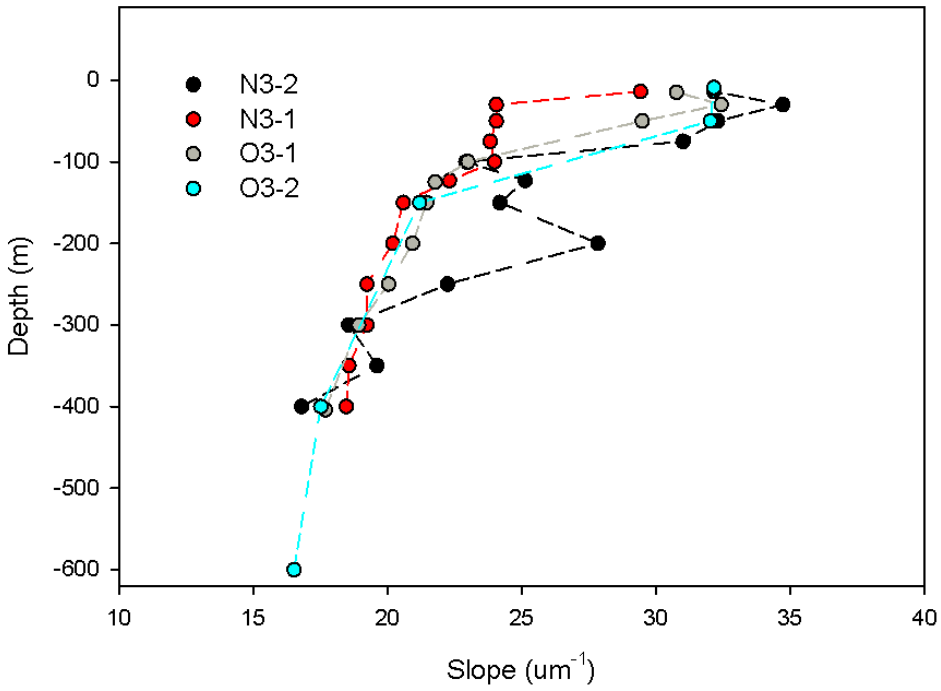

Figure 3.9 Slope (um^{-1}) with depth at three stations during 2013 near the DWH site.

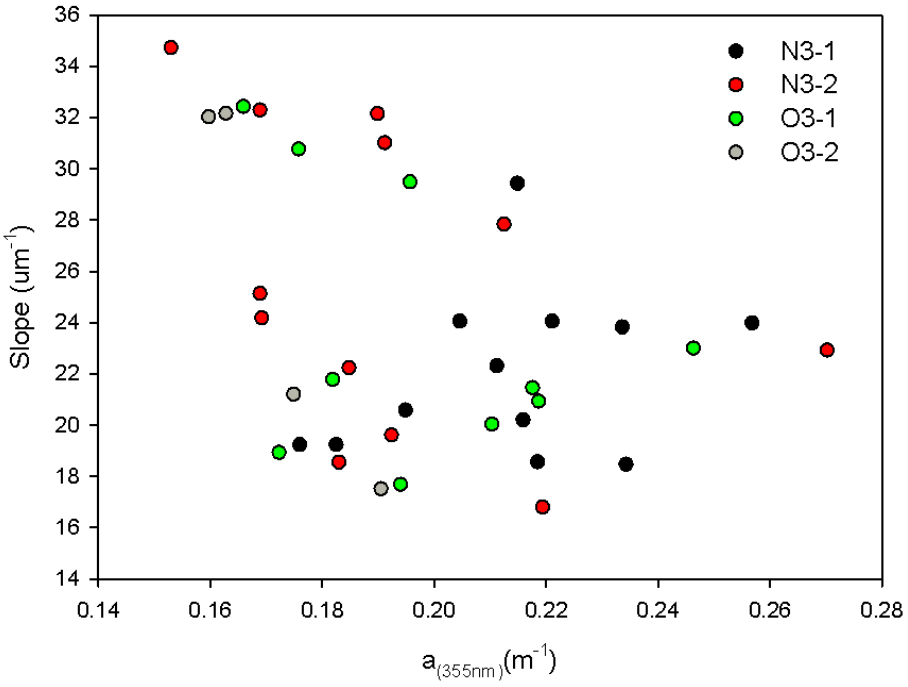

Figure 3.10 Spectral slope variations as a function of absorption.

The spectral slope plotted as a function of depth clearly shows highest slope values in the surface and near-surface water of the study site (Figure 3.9). Spectral slope is then observed to decrease with depth and is the lowest at the greatest depth. High levels of spectral slope in surface waters suggest the strong role of photo-oxidation in the surface waters. Low values of spectral slope at depths suggest greater biological degradation of CDOM. Relationship between CDOM absorption and spectral slope shows a general trend of decreasing slope with increasing absorption (Figure 3.10). Different water masses, CDOM photo-oxidation likely contributed to the variability in the relationship.

3.3.3 CDOM Fluorescence

Fluorescence spectroscopy technique using EEMs (excitation-emission matrices) (Coble et al., 1990) has been widely applied to investigate and identify DOM sources in various natural waters (Coble 1996, 1998). EEMs at the nearshore station N3-1 from surface to bottom at 15m, 30m, 50m, and 400m depths, respectively demonstrate the presence of various fluorophores in the seawater at various relative concentrations (Figure 3.11). Some of the main fluorophores previously identified (Table 3.1; Coble et al. 1996) that can be visually seen present in the water column near the DWH site (Table 3.2) are the humic-like A, the marine-like M, the protein-like T and B fluorophores (Figure 3.11). The relative intensities of the fluorescence peaks however vary at different depths suggesting different influences on the CDOM fluorescent components.

For a large EEMs dataset, the application of the statistical tool parallel factor analysis (PARAFAC) aids in effectively modeling the EEMs and in quantifying the concentration of individual components. PARAFAC was applied to the EEM dataset (28 samples for the 2013 cruise) with some analytical and statistical assumptions (Stedmon et al. 2008). Split-half analysis and analysis of residuals and loadings were applied to determine the number of components present in the EEM data (Stedmon et al. 2003).

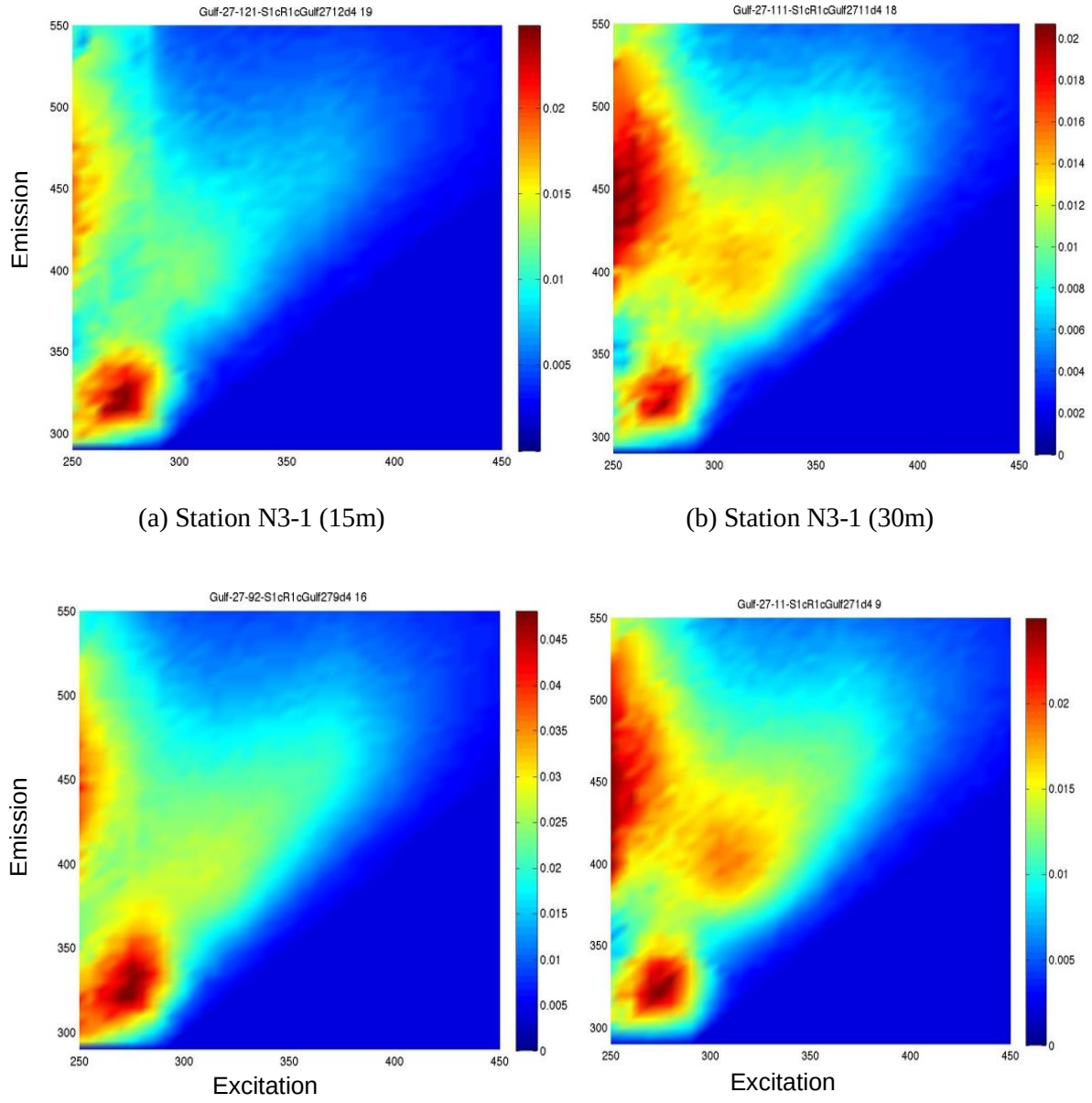

(a) Station N3-1 (15m) (b) Station N3-1 (30m)

(c) Station N3-1 (50m) (d) Station N3-1 (400m)

Figure 3.11 EEMs spectra of samples obtained at station N3-1 at 15m, 30m, 50m and 400m depth.

The PARAFAC model was tested with different number of components. The calculated residual plots for 3, 4 and 5 component models indicate that the four components model resulted in minimum residuals (Figure 3.12) for the dataset. Mean squared error (MSE) is seen to be the least for the four component model suggesting that the four components model is well represented for the EEMs data used in this analysis.

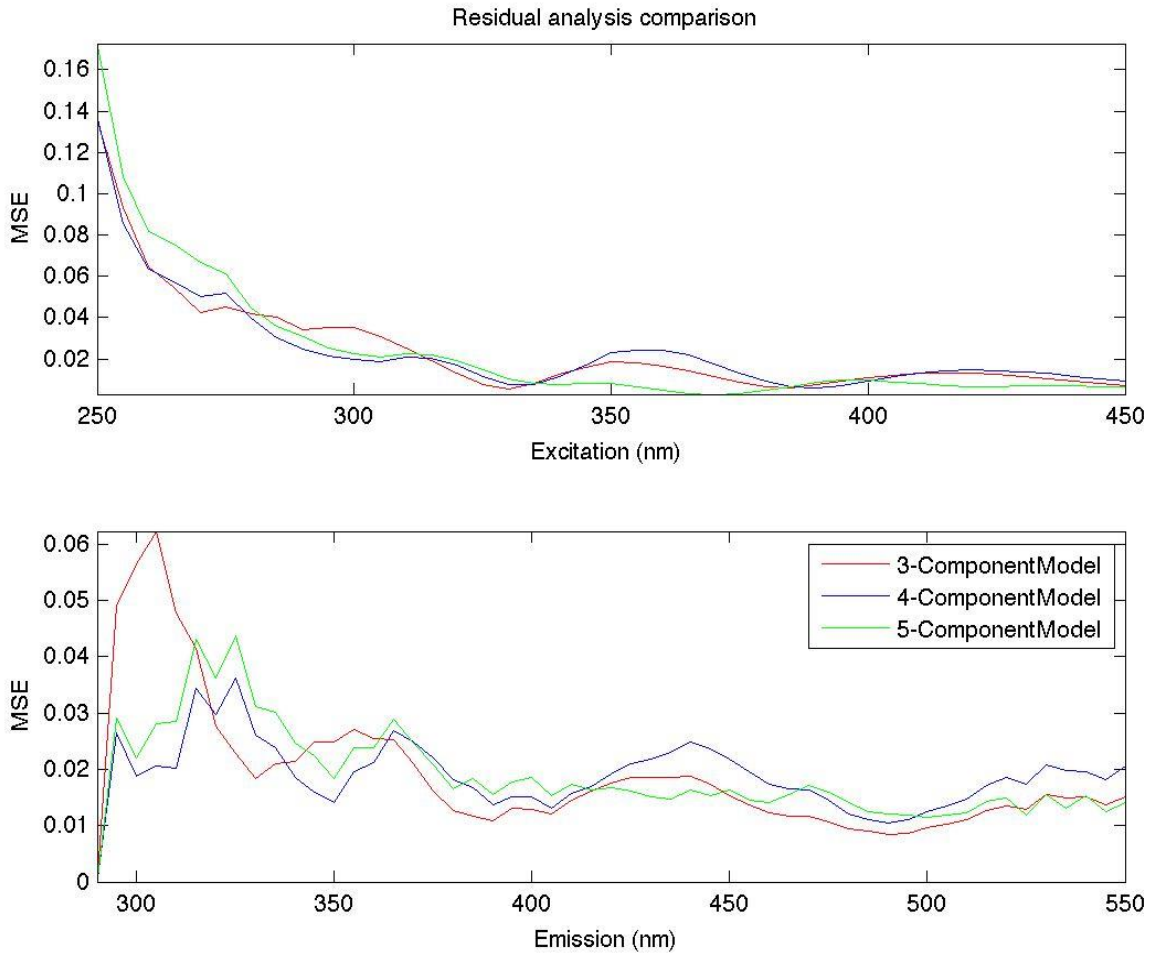

Figure 3.12 Comparison of residual analysis and mean square error between 3, 4 and 5 component model.

Table 3.2 Positions of fluorescence maxima of the four identified components

Component	Excitation Maxima(nm)	Emission Maxima (nm)
Component 1	260(375)	475
Component 2	320(<250)	400
Component 3	275	340
Component 4	260	310

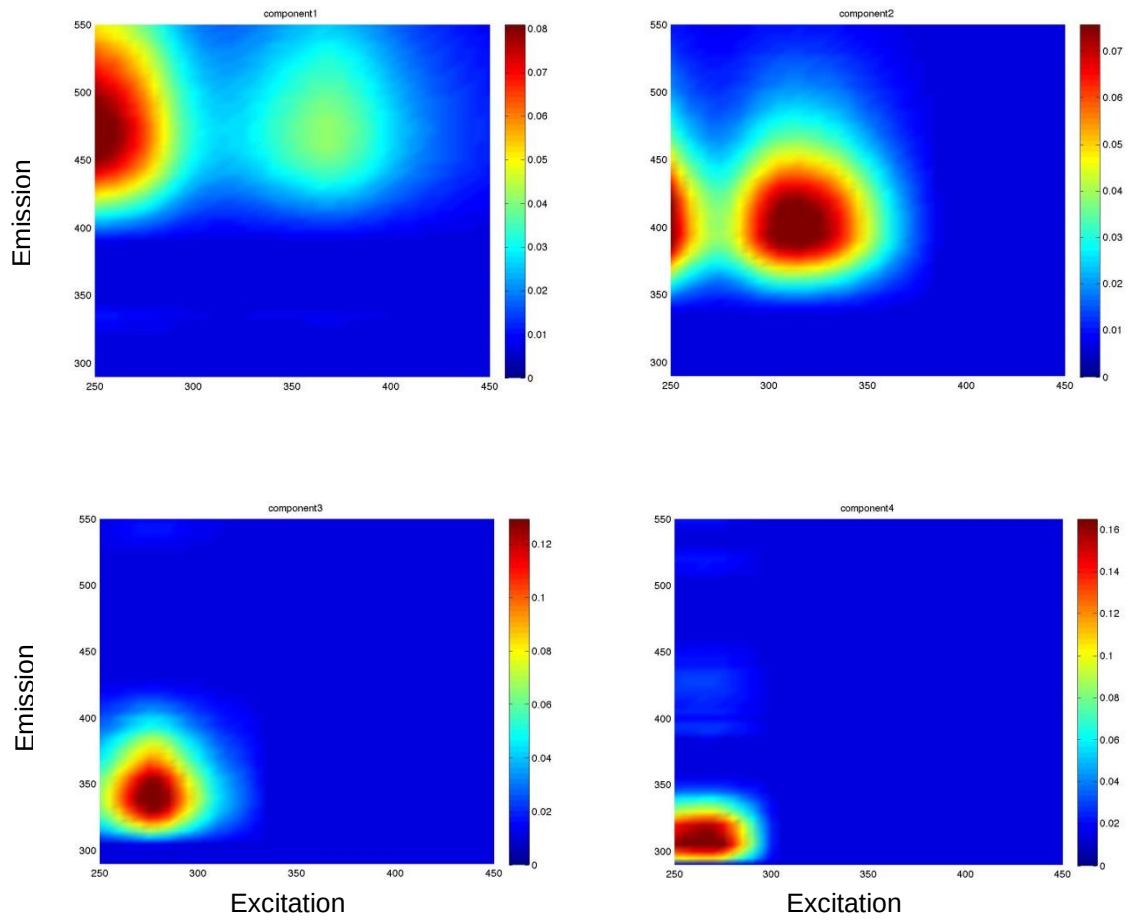

Figure 3.13 The four components determined using the PARAFAC model

The four components (Figure 3.13) and the positions of fluorescence maxima of these components identified by PARAFAC analysis (Table 3.2) indicate the components are similar to the previously identified components in oceanic waters (Coble et al. 1996; Stedmon et al. 2007). Component 1 has a primary (and secondary) fluorescence peak at an excitation/emission wavelength of 260 (375) nm/475 nm. The primary and secondary fluorescence peaks for component 2 occurred at 320(<250)/400 nm. Component 3 has a strong single fluorescence peak occurring at 275/340 nm, while component 4 fluorescence peak was identified at 260/310 nm excitation/emission wavelength (Table 3.2). These components do not appear to correspond to the oil fluorescent signatures detected near the DWH the oil spill event in 2010 (Zhou et al. 2013).

Component 1 is similar to humic-like A peak (Table 3.3) and has been shown to be of terrestrial origin and identified in other studies as Component 1 (Kowalczuk et al., 2009), Component 3 (Stedmon et al., 2003), Component 1 (Stedmon and Markager, 2005), Component 2 (Hua et al., 2007) and Component 1 (Ohno and Bro, 2006). Component 2 is similar to M peak and is comprised of marine humic-like fluorescence substance mainly produced by local biological activity (Coble 1996, 1998; Zepp et al. 2004; Bissett et al. 2005). Component 3 is similar to T peak or Tryptophan-like, protein-like substance. Component 4 is similar to B peak with a peak at 275/310 nm and is associated with tyrosine-like, protein like substance. Tyrosine-like and protein-like organic material are mostly derived from micro decomposition of algae, phytoplankton and bacteria in marine waters (Coble 1996; Yamashita et al. 2008).

Table.3.3 Components in this study and corresponding major fluorophores found in bulk seawater.

Components In this study	Ex_{max}(nm)	Em_{max}(nm)	EEMs peak, Coble et al. 1996
Component 1	260	380-460	A, Humic-like
Component 2	312	380-420	M, Marine humic-like
Component 3	275	340	T, Tryptophan-like, protein like
Component 4	275	310	B, Tyrosine-like, protein like

The component scores (related to the concentration of the fluorophores) of the four components obtained from PARAFAC analysis indicate the humic-like material to form a major component of the fluorescent DOM near the DWH site (Figure 3.14; Table 3.4). On average, Component1 has the largest magnitude (mean 0.22) followed by Component 2 (mean 0.17), Component 3 (mean 0.11) and Component 4 (mean 0.08) with the lowest concentration. However, at the nearshore stations N3-1 and to a lesser extent the station N3-2 that were influenced by the shelf plume (Figure 2.3), the intensity of the humic-like and protein-like fluorophores were higher than the two offshore stations. This suggests that eddy activity associated with Loop Current may be an important mechanism for dispersal of organic

material to the oligotrophic waters in the northern Gulf of Mexico. In addition, the much higher levels of protein-like Components 3 and 4 across the water column for the nearshore stations N3-1 and N3-2 indicate that biologically derived organic material are likely the main fluxes of organic material to the deeper waters near the DWH site.

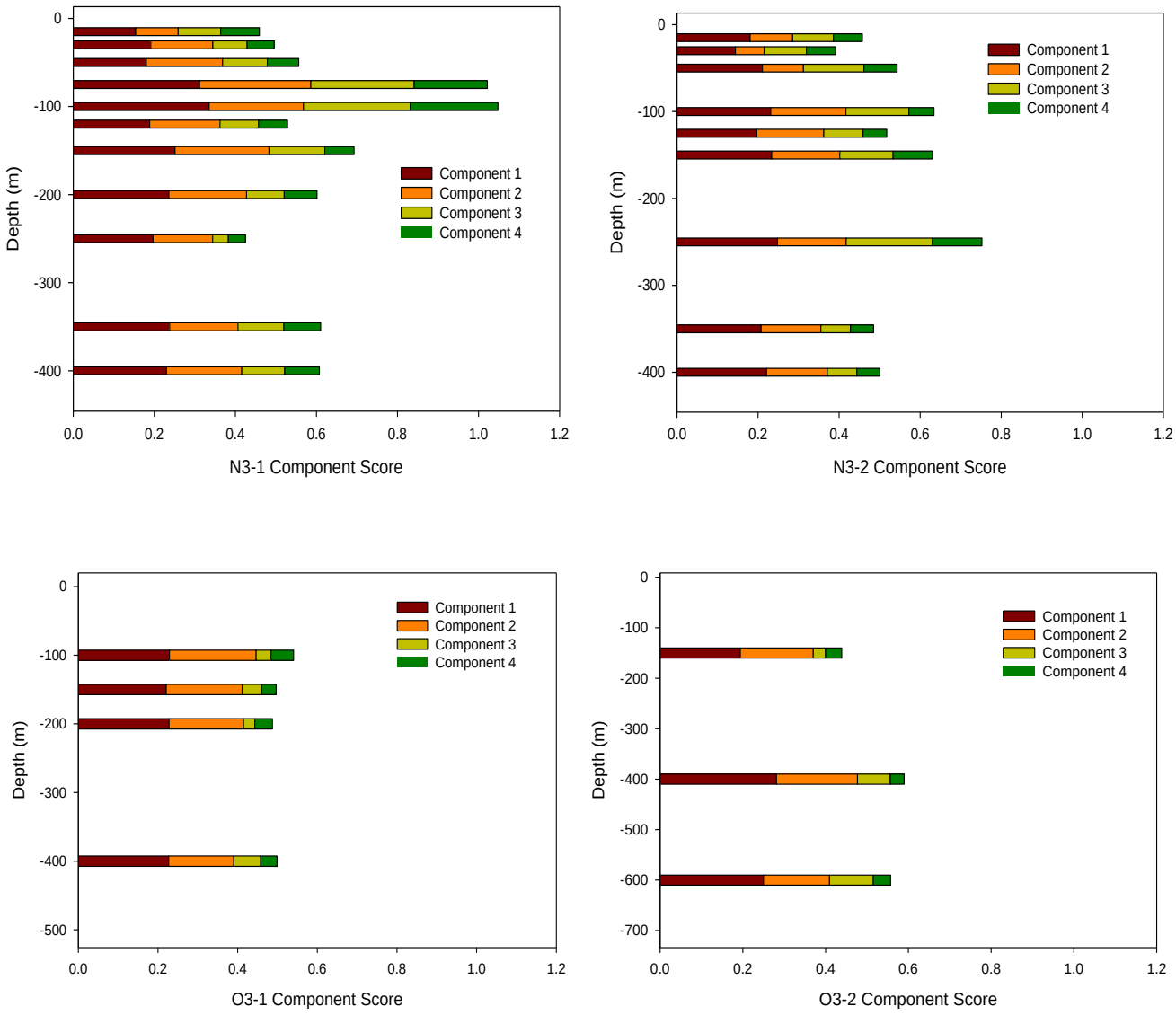

Figure 3.14 Fluorescence components distribution with depth at the four stations near the DWH site during the 2013 cruise.

Table 3.4 CDOM fluorescent component scores at the four sampling stations identified by PARAFAC analysis.

Sample	Component1	Component2	Component3	Component4
Station N3-1 (Depth m)				
-30	0.1913	0.1531	0.0848	0.0663
-50	0.1804	0.1883	0.1102	0.0775
-75	0.3117	0.2744	0.2552	0.1805
-100	0.3354	0.2327	0.2635	0.2163
-120	0.1885	0.1735	0.0953	0.0716
-150	0.2509	0.232	0.1377	0.0723
-200	0.236	0.1916	0.093	0.0808
-250	0.1968	0.1472	0.0387	0.0422
-350	0.238	0.1684	0.1132	0.0909
-400	0.2301	0.1859	0.1057	0.0858
Station N3-2 (Depth m)				
-15	0.1806	0.1048	0.1007	0.0715
-30	0.1442	0.0709	0.1045	0.0719
-50	0.2108	0.1011	0.1493	0.082
-100	0.2313	0.1857	0.1552	0.062
-125	0.1972	0.1651	0.0967	0.0586
-150	0.2338	0.168	0.1315	0.0973
-250	0.2481	0.1696	0.2122	0.1225
-350	0.2077	0.1475	0.0732	0.0567
-400	0.2211	0.15	0.073	0.0566
Station O3-1 (Depth m)				
-100	0.2287	0.2179	0.0373	0.0564
-150	0.2208	0.1905	0.0491	0.0362
-200	0.228	0.1869	0.0284	0.0441
-400	0.2269	0.1634	0.0675	0.041
Station O3-2 (Depth m)				
-150	0.194	0.1764	0.0296	0.0392
-400	0.2812	0.196	0.0793	0.0334
-600	0.2498	0.1599	0.1055	0.042

Chapter 4 Summary

The physical properties in the ocean water, DOC concentrations, CDOM optical properties and parallel factor analysis have been used in this thesis to study the CDOM spectral absorption and fluorescence properties near the Deepwater Horizon site following the spill. The results of study could serve to provide a measurement component to monitor the northern Gulf of Mexico for potential effects of the DWH accident on the seawater biogeochemical properties including DOM/CDOM optical properties, to understand the CDOM composition, distribution and relationship between environmental factors three years after the largest oil spill in U.S. waters. The major findings of this study are:

- Loop Current and its eddies play an important role in determining the physical properties of study area near DWH site, such as temperature and salinity.
- Chlorophyll fluorescence and concentrations of dissolved oxygen appeared similar likely suggesting similar levels of dissolved organic material near the DWH site during the two survey years.
- The vertical distributions of DOC concentrations which exhibited larger values in the surface mixed layer and decreased with depth, are likely related to higher biological productivity in these waters.
- Generally, CDOM absorptions are higher and have greater rate of decrease in absorption at all the four stations spectra at 15 m and 100 m. CDOM levels appear lower for the two offshore stations (O3-1 and O3-2) than the inner stations (N3-1, N3-2). CDOM absorption peaks observed at ~100 m correspond to elevated chlorophyll fluorescence suggesting a biological source of CDOM at this depth. The pattern of CDOM-salinity relationship is not clear in comparison to coastal and river dominated waters.
- The spectral slope showed a clear decrease in slope values with increasing depth, which could be attributed to photo-oxidation that results in CDOM loss and biological degradation of CDOM.

- The application of the statistical tool parallel factor analysis (PARAFAC) identified four CDOM fluorescence components in samples.
- Component 1 is terrestrial origin humic-like substance and component 2 is marine origin humic-like substance mainly produced by local biological activity. Two protein-like components, Components 3 and 4 are mostly derived from micro decomposition of algae, phytoplankton and bacteria in marine waters.
- Humic substances were a major contributor to the CDOM pool in study area.
- Influence of terrestrial input and eddy activity associated with Loop Current have been observed at the study site and CDOM composition shows no oil signature three years after the Deepwater Horizon oil spill.

References

Bissett, W. P., Arnone, R., DeBra, S., Dieterle, D. A., Dye, D., Kirkpatrick, G. J., and Vargo, G. A., 2005. Predicting the optical properties of the West Florida Shelf: resolving the potential impacts of a terrestrial boundary condition on the distribution of colored dissolved and particulate matter. Marine chemistry,95(3), 199-233.

Blough, N. V., and Green, S. A., 1995. Spectroscopic characterization and remote sensing of non-living organic matter. The Role of Non-living Organic Matter in the Earth's Carbon Cycle (RG Zepp and C. Sonntag, eds.), John Wiley & Sons Ltd, 23-45.

Bro, R., 1997. PARAFAC. Tutorial and applications. Chemometrics and Intelligent Laboratory Systems; 38 (2): 149-171.

Camilli, R., Reddy, C. M., Yoerger, D. R., Van Mooy, B. A., Jakuba, M. V., Kinsey, J. C., and Maloney, J. V., 2010. Tracking hydrocarbon plume transport and biodegradation at Deepwater Horizon. Science, 330(6001), 201-204.

Cho, K., Reid, R. O., and Nowlin, W. D., 1998. Objectively mapped stream function fields on the Texas - Louisiana shelf based on 32 months of moored current meter data. Journal of Geophysical Research: Oceans (1978–2012), 103(C5), 10377-10390.

Christensen, J. H., Hansen, A. B., Mortensen, and J., Andersen, O., 2005. Characterization and matching of oil samples using fluorescence spectroscopy and parallel factor analysis. Anal. Chem. 77 (7), 2210–2217.

Coble, P. G., 1996. Characterization of marine and terrestrial DOM in seawater using excitation-emission matrix spectroscopy. Marine Chemistry 51 (4): 325-346.

Coble, P. G., 2007. Marine Optical Biogeochemistry: The Chemistry of Ocean Color. Chemical Reviews 107: 402-418.

Coble, P. G., Del Castillo, C. E., and Avril, B., 1998. Distribution and optical properties of CDOM in the Arabian Sea during the 1995 Southwest Monsoon. Deep-Sea Research II 45: 2195– 2223.

Coble, P. G., Green, S. A., Blough, N. V., and Gagosian, R. B., 1990. Characterization of dissolved organic matter in the Black Sea by fluorescence spectroscopy. Nature (348): 432-435.

Dagg, A. I., 1999. Responsible animal-based research: Three flags to consider. Journal of Applied Animal Welfare Science, 2(4), 337-346.

Del Castillo, C. E., and Coble P. G., 2000. Seasonal variability of the colored dissolved organic matter during the 1994–95 NE and SW monsoons in the Arabian Sea. Deep-Sea Research 47: 1563–1579.

Del Castillo, C. E., Coble, P. G., Morel, J. M., Lopez, J. M., and Corredor, J. E., 1999. Analysis of the optical properties of the Orinoco River Plume by absorption and fluorescence spectroscopy. Marine Chemistry 66: 35-51.

Del Vecchio, R., and Blough, N. V., 2004. On the origin of the optical properties of humic substances. Environmental Science and Technology 38: 3885–3891.

Del Vecchio, R., and Blough, N. V., 2006. Influence of Ultraviolet Radiation on the Chromophoric Dissolved Organic Matter in Natural Waters. In Environmental UV Radiation: Impact on Ecosystems and Human Health and Predictive Models, eds. F. Ghetti, G. Checcucci, and J.F. Bornman, 203-216, Springer, printed in the Netherlands.

D'Sa, E. J., and DiMarco, S. F., 2009. Seasonal variability and controls on chromophoric dissolved organic matter in a large river-dominated coastal margin. Limnology and Oceanography, 54: 22332242.

D'Sa, E. J., Steward R. G., Vodacek A., Blough N. V., and Phinney D., 1999. Optical absorption of seawater colored dissolved organic matter determined using a liquid capillary waveguide. Limnology and Oceanography, 44: 1142-1148.

Gulf of Mexico Fact Sheet, http://www.eia.gov/. 20 Nov. 2013.

Guo, L., Santschi, P. H., and Warnken, K. W., 1995. Dynamics of dissolved organic carbon (DOC) in oceanic environments. Limnology and Oceanography, 40(8), 1392-1403.

Guo, L., White, D. M., Xu, C., and Santschi, P. H., 2009. Chemical and isotopic composition of high-molecular-weight dissolved organic matter from the Mississippi River plume. Marine Chemistry, 114(3), 63-71.

Harvey, G. R., and Boran D. A., 1985. The geochemistry of humic substances in seawater. In Humic substances in Soil, Sediment, and Water. Wiley-Interscience, 233-247.

Helms, J. R., Stubbins, A., Ritchie, J. D., Minor, E. C., Kieber, D. J., and Mopper, K., 2008. Absorption spectral slopes and slope ratios as indicators of molecular weight, source, and photobleaching of chromophoric dissolved organic matter. Limnology and Oceanography, 53(3), 955.

Hofmann, E. E., and Worley, S. J., 1986. An investigation of the circulation of the Gulf of Mexico. Journal of Geophysical Research, 91(C12), 14221-14.

Holbrook, R. D., Yen J. H., and Grizzard T. J., 2006. Characterizing natural organic material from the Occoquan Watershed (Northern Virginia, US) using fluorescence spectroscopy and PARAFAC. Science of the Total Environment 361: 249-266.

Hua, B., Dolan, F., McGhee, C., Clevenger, T. E., and Deng, B., 2007. Water-source characterization with fluorescence EEM spectroscopy: PARAFAC analysis. International Journal of Environmental Analytical Chemistry; 87 (2): 135-147.

Johnson, D. R., 2008. Ocean surface current climatology in the Northern Gulf of Mexico. Published by the Gulf Coast Research Laboratory, Ocean Springs, Mississippi.

Kowalczuk, P., Durako M. J., Young, H., Kahn, A. E., Cooper, W. J., and Gonsior, M., 2009. Characterization of dissolved organic matter fluorescence in the South Atlantic Bight with use of PARAFAC model: Interannual variability. Marine Chemistry; doi: 10.1016/j/marchem.2009.01.015.

Kujawinski, E. B., Kido Soule, M. C., Valentine, D. L., Boysen, A. K., Longnecker, K., and Redmond, M. C., 2011. Fate of dispersants associated with the Deepwater Horizon oil spill. Environmental Science & Technology, 45(4), 1298-1306.

Leben, R. R., Born H., and Engebreth B. R., 2002. Operational altimeter data processing for mesoscale monitoring. Marine Geodesy, 25, 3-18.

Lin, Q., and Mendelssohn, I. A., 2012. Impacts and recovery of the Deepwater Horizon oil spill on vegetation structure and function of coastal salt marshes in the Northern Gulf of Mexico. Environmental Science & Technology, 46(7), 3737-3743.

Markager, S., and Vincent W. F., 2000. Spectral light attenuation and the absorption of UV and blue light in natural waters. Limnology and Oceanography 45: 642-650.

Mascarelli, A., 2010. Deepwater Horizon: After the oil. Nature, 467(7311), 22.

Mendelssohn, I. A., Andersen, G. L., Baltz, D. M., Caffey, R. H., Carman, K. R., Fleeger, J. W., and Rozas, L. P., 2012. Oil impacts on coastal wetlands: implications for the Mississippi River Delta ecosystem after the Deepwater Horizon oil spill. BioScience, 62(6), 562-574.

Mendoza, W. G., Riemer, D. D., and Zika, R. G., 2013. Application of fluorescence and PARAFAC to assess vertical distribution of subsurface hydrocarbons and dispersant during the Deepwater Horizon oil spill. Environ. Sci.: Processes Impacts, 15(5), 1017-1030.

Miller, R. L., Belz, M., Castillo, C. D., and Trzaska, R., 2002. Determining CDOM absorption spectra in diverse coastal environments using a multiple pathlength, liquid core waveguide system. Continental Shelf Research, 22(9), 1301-1310.

Milliman, J. D., and Meade, R. H., 1983. World-wide delivery of river sediment to the oceans. The Journal of Geology, 1-21.

Mitra, S., et al. 2012. Macondo-1 well oil-derived polycyclic aromatic hydrocarbon in mesozooplankton from the northern Gulf of Mexico. Geophysical Research Letters, 39, L01605, doi:10.1029/2011GL049505.

Morel, A., Claustre, H., Antoine, D., and Gentili, B., 2007. Natural variability of bio-optical properties in Case1waters: attenuation and reflect ance with in the visible and near-UV spectral domains,

as observed in South Pacific and Mediterranean waters. Biogeosciences Discussions 4,2147–2178.

Morey, S. L., Martin, P. J., O'Brien, J. J., Wallcraft, A. A., and Zavala‐Hidalgo, J., 2003. Export pathways for river discharged fresh water in the northern Gulf of Mexico. Journal of Geophysical Research: Oceans (1978–2012), 108(C10).

Morrison, J. M., and Nowlin, W. D., 1982. Repeated nutrient, oxygen, and density sections through the Loop Current. Journal of Marine Research 35, 105-128.

Nababan, B., Muller-Karger, F. E., Hu, C., and Biggs, D. C., 2011. Chlorophyll variability in the northeastern Gulf of Mexico. International Journal of Remote Sensing, 23, 8373-8391.

Nelson, N. B., Carlson, C. A., and Steinberg, D. K., 2004. Production of chromophoric dissolved organic matter by Sargasso Sea microbes. Marine Chemistry 89, 273–287.

Nelson, N. B., Siegel, D. A., Carlson, C. A., Swan, C., Smethie, W. M., and Khatiwala, S., 2007. Hydrography of chromophoric dissolved organic matter in the North Atlantic. Deep-Sea Research 54, 710–731.

NRC. 2005. Oil Spill Dispersants: Efficacy and Effects; National Academy of Sciences. Web. 20 Nov. 2013.

Ohno, T., 2002. Fluorescence Inner-Filtering Correction for Determining the Humification Index of Dissolved Organic Matter. Environmental Science and Technology, 36: 742-746.

Reddy, K. R., and DeLaune R. D., 2008. Biogeochemistry of Wetlands: Science and Applications. Printed in New York, pp 806: CRC press.

Schrope, M., 2011. Deep wounds. Nature, 472(7342), 152-154.

Shank, G. C., and Evans, A., 2011. Distribution and photoreactivity of chromophoric dissolved organic matter in northern Gulf of Mexico shelf waters. Continental Shelf Research, 31(10), 1128-1139.

Singh, S., D'Sa, E. J., and Swenson, E. M., 2010. Chromophoric dissolved organic matter (CDOM) variability in Barataria Basin using excitation–emission matrix (EEM) fluorescence and parallel factor analysis (PARAFAC). Science of the Total Environment, 408(16), 3211-3222.

Solis, R. S., and Powell, G. L., 1999 . Hydrography, mixing characteristics, and residence times of Gulf of Mexico estuaries. Biogeochemistry of Gulf of Mexico estuaries, 29-61.

Stedmon, C. A., and Bro, R., 2008. Characterizing dissolved organic matter fluorescence with parallel factor analysis: a tutorial. Limnology Oceanography: Methods, 6, 572-579.

Stedmon, C. A., and Markager S., 2005. Tracing the production and degradation of autochthonous fractions of dissolved organic matter using fluorescence analysis. Limnology and Oceanography 50 (5): 1415-1426.

Stedmon, C. A., Markager, S., and Bro. R., 2003. Tracing dissolved organic matter in aquatic environments using a new approach to fluorescence spectroscopy. Marine Chemistry 82: 239-254.

Stedmon, C. A., Thomas D. N., Granskog M., Kaartokallio H., Papadimitriou S., and Kuosa H., 2007. Characteristics of Dissolved Organic Matter in Baltic Coastal Sea ice: Allochthonous or Autochthonous Origins? Environmental Science and Technology 41: 7273-7279.

Sturges, W., 1993. The annual cycle of the western boundary current in the Gulf of Mexico. Journal of Geophysical Research: Oceans (1978–2012), 98(C10), 18053-18068.

Sturges, W., and Leben, R., 2000. Frequency of ring separations from the Loop Current in the Gulf of Mexico: A revised estimate. Journal of Physical Oceanography, 30(7), 1814-1819.

Tedetti, M., Guigun, C., and Goutx, M., 2010. Utilization of a submersible UV fluorometer for monitoring anthropogenic inputs in the Mediterranean coastal waters. Marine Pollution Bulletin, 60, 530-362.

U.S. scientific teams refine estimates of oil flow from BP's well prior to capping. 2010. Gulf of Mexico Oil Spill Response.

Vodacek, A., Blough,N. V., DeGrandpre, M. D., Peltzer, E. T., and Nelson, R. K., 1997. Seasonal variation of CDOM and DOC in the Middle Atlantic Bight: terrestrial inputs and photooxidation. Limnology and Oceanography 42, 674–686.

Walker, N. D., Pilley, C. T., Raghunathan, V. V., D'Sa, E. J., Leben, R. R., Hoffmann, N. G., and Turner, R. E., 2011. Impacts of Loop Current frontal cyclonic eddies and wind forcing on the 2010 Gulf of Mexico oil spill. Monitoring and Modeling the Deepwater Horizon Oil Spill: A Record-Breaking Enterprise, 103-116.

Walker, N. D., and Rabalais, N. N., 2006. Relationships among satellite chlorophylla, river inputs, and hypoxia on the Louisiana Continental shelf, Gulf of Mexico. Estuaries and Coasts, 29(6), 1081-1093.

Welsh, S. E., and Inoue, M., 2000. Loop Current rings and the deep circulation in the Gulf of Mexico. Journal of Geophysical Research: Oceans (1978–2012), 105(C7), 16951-16959.

Yamashita, Y., and Tanoue, E., 2008. Production of bio-refractory fluorescent dissolved organic matter in the ocean interior. Nature Geoscience, 1, 579–582.

Zepp, R. G., Baughman, G. L., and Schlotzhauer, P. F., 1981. Comparison of photochemical behavior of various humic substances in water: I. Sunlight induced reactions of aquatic pollutants photosensitized by humic substances. Chemosphere, 10(1), 109-117.

Zepp, R. G., Sheldon, W. M., and Moran, M. A., 2004. Dissolved organic fluorophores in southeastern US coastal waters: correction method for eliminating Rayleigh and Raman scattering peaks in excitation–emission matrices. Marine Chemistry, 89: 15–36.

Zhou, Z., Guo, L., Shiller, A. M., Lohrenz, S. E., Asper, V. L., and Osburn, C. L., 2012. Characterization of oil components from the Deepwater Horizon oil spill in the Gulf of Mexico using fluorescence EEM techniques. Marine Chemistry, 148: 10-21.

Vita

Zhi Li was born in 1987, in XinGan, Jiangxi Province, China. He graduated from XinGan High School in 2005. Zhi Li attended Ocean University of China in September, 2005, and obtained a degree of Bachelor of Science in Chemistry in June, 2009. He then joined Guangxi Mangrove Research Center as a Research Assistant and served there for two and half years before joining Louisiana State University, USA in Summer, 2012. Presently, he is a candidate for the degree of Master in Science in the Department of Oceanography and Coastal Sciences, Louisiana State University.